Article

Cell Reports

ppGpp Controls Global Gene Expression in Light and in Darkness in *S. elongatus*

Graphical Abstract

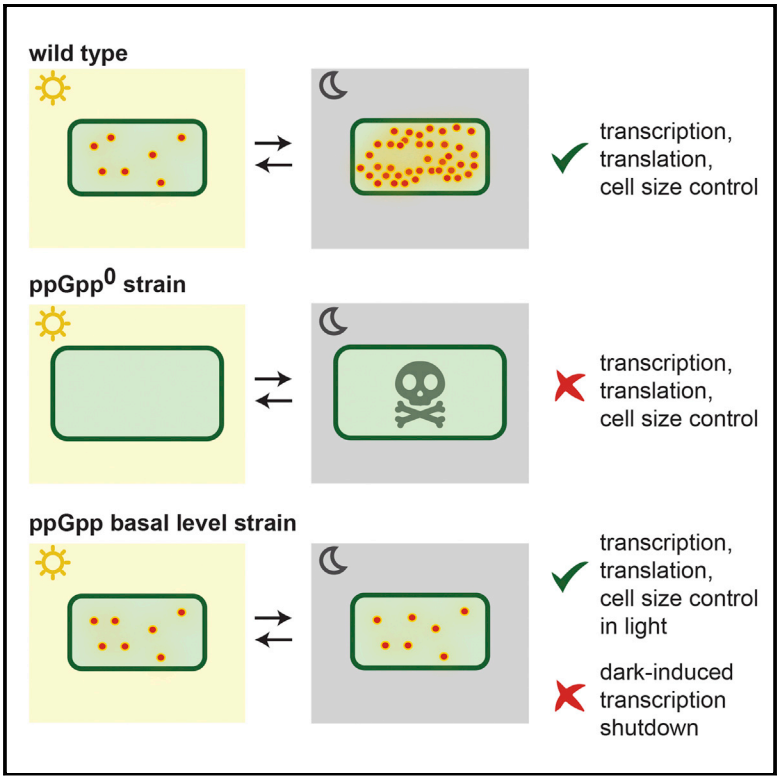

Authors

Anna M. Puszynska, Erin K. O'Shea

Correspondence

osheae@hhmi.org

In Brief

Puszynska and O'Shea characterize the role of the signaling molecule ppGpp in regulation of the physiology of *Synechococcus elongatus*. They find that basal levels of ppGpp control transcription, translation, and cell size in light and protect cell viability in darkness, and they show that ppGpp accumulation is required for dark-induced transcriptional shutdown.

Highlights

- (p)ppGpp regulates the physiology of *S. elongatus* in light and in darkness
- Basal levels of (p)ppGpp regulate transcription, translation, and cell size in light
- Basal levels of ppGpp are sufficient to protect cell viability in the dark
- (p)ppGpp accumulation is required for dark-induced transcriptional shutdown

Data and Software Availability

GSE10360

Puszynska & O'Shea, 2017, Cell Reports *21*, 3155–3165
December 12, 2017
https://doi.org/10.1016/j.celrep.2017.11.067

CellPress

Cell Reports
Article

ppGpp Controls Global Gene Expression in Light and in Darkness in *S. elongatus*

Anna M. Puszynska[1,2,3] and Erin K. O'Shea[1,2,3,4,5,*]
[1]Howard Hughes Medical Institute, Chevy Chase, MD, USA
[2]Department of Molecular and Cell Biology, Harvard University, Cambridge, MA 02138, USA
[3]Faculty of Arts and Sciences Center for Systems Biology, Harvard University, Cambridge, MA 02138, USA
[4]Department of Chemistry and Chemical Biology, Harvard University, Cambridge, MA 02138, USA
[5]Lead Contact
*Correspondence: osheae@hhmi.org
https://doi.org/10.1016/j.celrep.2017.11.067

SUMMARY

The bacterial and plant stringent response involves production of the signaling molecules guanosine tetraphosphate and guanosine pentaphosphate ((p)ppGpp), leading to global reorganization of gene expression. The function of the stringent response has been well characterized in stress conditions, but its regulatory role during unstressed growth is less studied. Here, we demonstrate that (p)ppGpp-deficient strains of *S. elongatus* have globally deregulated biosynthetic capacity, with increased transcription rate, translation rate, and cell size in unstressed conditions in light and impaired viability in darkness. Synthetic restoration of basal guanosine tetraphosphate (ppGpp) levels is sufficient to recover transcriptional balance and appropriate cell size in light and to rescue viability in light/dark conditions, but it is insufficient to enable efficient dark-induced transcriptional shutdown. Our work underscores the importance of basal ppGpp signaling for regulation of cyanobacterial physiology in the absence of stress and for viability in energy-limiting conditions, highlighting that basal (p)ppGpp level is essential in cyanobacteria in the environmental light/dark cycle.

INTRODUCTION

The nucleotides guanosine tetraphosphate (ppGpp) and guanosine pentaphosphate (pppGpp), collectively known as (p)ppGpp, are intracellular signals of a bacterial stress response pathway known as the stringent response (Cashel and Gallant, 1969; Potrykus and Cashel, 2008). These alarmones rapidly accumulate in bacterial cells exposed to nutritional and environmental stresses (Hauryliuk et al., 2015) and lead to global transcriptional reprogramming, curtailing expression of genes responsible for growth and division and inducing transcripts involved in resistance to stress and starvation (Potrykus and Cashel, 2008; Srivatsan and Wang, 2008; Hauryliuk et al., 2015). The stringent response also targets many metabolic enzymes that directly bind (p)ppGpp, further modifying cell physiology to adapt to adverse environmental changes (Kanjee et al., 2012).

In various bacteria, elevated (p)ppGpp levels play a crucial role in regulation of virulence, biofilm formation, motility, competence, antibiotic resistance, differentiation, and DNA damage repair (Boutte and Crosson, 2013; Kamarthapu et al., 2016). Moreover, (p)ppGpp accumulates in chloroplasts, thereby regulating stress resistance in plants (van der Biezen et al., 2000; Takahashi et al., 2004), which emphasizes the widespread importance of stringent response signaling in nature. Although (p)ppGpp has been broadly studied in a variety of organisms as an effector of adaptation to adverse conditions, its function in controlling cell physiology in unstressed conditions has been less investigated (Gaca et al., 2015). It has been established that in the absence of stress, (p)ppGpp alarmones are the key molecules controlling growth rate in *E. coli* through regulation of rRNA synthesis (Sokawa et al., 1975; Ryals et al., 1982; Sarubbi et al., 1988; Potrykus et al., 2011) and that basal (p)ppGpp levels modulate amino acid and nucleotide metabolism in *Firmicutes* (Kriel et al., 2012; Gaca et al., 2013, 2015).

The key enzymes involved in the metabolism of (p)ppGpp are highly conserved and belong to the Rel/SpoT homolog (RSH) superfamily, named based on sequence homology to RelA and SpoT enzymes from *E. coli* (Atkinson et al., 2011). RelA is a (p)ppGpp synthetase associated with the ribosome; it senses amino acid deficiency by monitoring the ratio of charged to uncharged tRNAs during translation elongation (Hauryliuk et al., 2015). SpoT is a bifunctional enzyme with weak (p)ppGpp synthetase activity and strong hydrolase activity under unstressed conditions (Hauryliuk et al., 2015). The balance of the two activities of SpoT is shifted in favor of (p)ppGpp synthesis in response to various stress signals, likely through protein-protein interaction with other factors (Battesti and Bouveret, 2006; Hauryliuk et al., 2015). Outside of γ- and β-proteobacteria, the bifunctional Rel/SpoT homolog is termed Rel (Atkinson et al., 2011).

Here, we used the cyanobacterium *Synechococcus elongatus* PCC7942 to shed light on the role of (p)ppGpp signaling in regulation of cell physiology both during unstressed growth and in response to energy limitation during exposure to darkness. Cyanobacteria are a uniquely positioned group of organisms—they are photosynthetic prokaryotes whose ancestors constituted the evolutionary precursors of modern chloroplasts (Douglas and Raven, 2003). Hence, they are well suited to provide insight

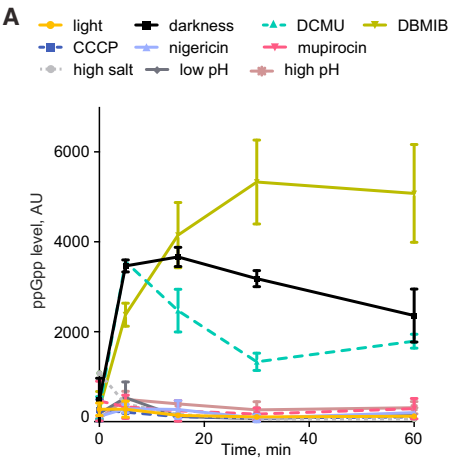

Figure 1. ppGpp Levels in Cells Exposed to Different Stresses and in Unstressed Conditions

(A) Levels of the nucleotide ppGpp measured by thin layer chromatography in cells subjected to a range of conditions: constant light, darkness, 10 μM 3-(3,4-dichlorophenyl)-1,1-dimethylurea (DCMU), 10 μM 2,5-dibromo-3-methyl-6-isopropylbenzoquinone (DBMIB), 50 μM nigericin, 10 μM carbonyl cyanide 3-chlorophenylhydrazone (CCCP), 10 μg/mL mupirocin, low pH (pH 4.0), high pH (pH 10.5), and high salt (250 mM NaCl). Points represent the mean of two independent experiments, with error bars displaying the SEM.

(B) Relative ppGpp levels in wild-type and the *rel*⁻ strain during a 12 hr exposure to darkness (top) and in constant light in unstressed conditions (bottom). Points represent the mean of two independent experiments, with error bars displaying the SEM.

See also Figure S1.

into the physiological relevance of (p)ppGpp signaling and other bacterial pathways that persisted in plants.

Complex signaling networks help align biological processes in *S. elongatus* with the environmental light/dark cycles (Smith, 1983). In the dark, cyanobacteria face deprivation of their external energy source, and (p)ppGpp has been shown previously to increase on exposure to darkness in these organisms (Doolittle, 1979; Surányi et al., 1987; Hood et al., 2016). The stringent response was proposed to be required for viability of *S. elongatus* cells in the dark (Hood et al., 2016). Here, we find that although induction of high levels of ppGpp is required for appropriate execution of global dark-induced transcriptional shutdown, low basal levels of ppGpp are critical for control of cell physiology during balanced growth in light and are sufficient to protect cell viability in response to darkness. Our results emphasize the role of light-responsive ppGpp signaling in global control of biosynthetic processes in steady-state conditions and under stress. We highlight the importance of the basal ppGpp level both in maintenance of metabolic balance and in persistence in adverse conditions, providing insight into regulation of cyanobacterial physiology.

RESULTS

(p)ppGpp Is Present at a Basal Level in Light and Accumulates in Response to Changes in Photosynthetic Activity

To determine whether accumulation of the alarmone ppGpp in cyanobacteria constitutes a specialized response to specific environmental cues or is a part of a general response to a range of stressors, we analyzed ppGpp levels in cultures exposed to various stress stimuli. We treated cells for 1 hr with darkness; with two inhibitors of the photosynthetic electron transport chain, 3-(3,4-dichlorophenyl)-1,1-dimethylurea (DCMU) and 2,5-dibromo-3-methyl-6-isopropylbenzoquinone (DBMIB) (acting, respectively, upstream and downstream of the plastoquinone pool); with agents disrupting membrane potential, carbonyl cyanide 3-chlorophenylhydrazone (CCCP) and nigericin; with mupirocin, which inhibits the activity of isoleucyl-tRNA synthetase, mimicking the effects of amino acid starvation; with high salt; and with extremes of pH. In agreement with previous reports (Doolittle, 1979; Hood et al., 2016), we observe that exposure to darkness induces rapid ppGpp accumulation in *S. elongatus* (Figure 1A). Treatment with the photosynthetic chain inhibitors DCMU and DBMIB also results in a strong increase in ppGpp levels, whereas other stressors do not significantly induce the synthesis of ppGpp. Thus, rapid ppGpp accumulation in cyanobacteria does not act as a general stress response but instead is triggered by changes in the activity or in the redox state of the components of the photosynthetic electron transport chain.

To gain insight into the changes in ppGpp levels in cells under physiologically relevant conditions, we analyzed levels of ppGpp during the light/dark cycle (12 hr of light and 12 hr of darkness) in entrained cultures of wild-type and in the *rel*⁻ strain, in which the gene *synpcc7942_1377*, encoding a bifunctional (p)ppGpp synthetase/hydrolase, was deleted. We observe that in wild-type cells exposed to dark, the initial rapid accumulation of ppGpp is followed by a slow decline, with ppGpp levels reaching a new steady state after approximately 3 hr (Figure 1B, top panel). In the *rel*⁻ strain, we do not observe any significant changes in ppGpp levels in response to darkness (Figure 1B, top panel; Figure S1A), which suggests that Rel is the key enzyme in *S. elongatus* responsible for production of the (p)ppGpp alarmones in response to darkness, in accordance with a report by Hood et al. (2016). We also observe that a point mutation that inactivates the synthetase activity of Rel (D297A, introduced based on Hogg et al., 2004) is sufficient to block ppGpp accumulation in response to darkness (Figure S1B), emphasizing the role of the enzymatic activity of Rel in the control of ppGpp levels. During the light period of the light/dark cycle, we find that ppGpp levels in wild-type cells are low yet remain consistently above the background levels detected in the *rel*⁻ strain (Figure 1B, bottom panel), indicating that ppGpp is present in cyanobacteria not only during stress but also at a basal level in unstressed conditions.

Basal Levels of ppGpp Are Crucial for Normal Cell Physiology in Light

Although the role of (p)ppGpp in regulation of transcription in response to adverse environmental cues has been studied in a variety of bacteria (Boutte and Crosson, 2013; Hauryliuk et al., 2015), its function in unstressed conditions during steady-state growth has remained less understood, prompting us to ask whether low concentrations of ppGpp elicit systemic effects on cyanobacterial physiology outside of stress. To determine whether the basal level of ppGpp during growth in constant light (unstressed conditions) affects transcriptional regulation, we compared gene expression in entrained cultures of the *rel*$^{-}$ strain and in wild-type by RNA sequencing. To ensure accurate inference of gene expression levels, we added exogenous RNA standards for normalization and factored in the number of cells harvested for RNA extraction using the relationship between optical density 750 (OD_{750}) and the cell number per milliliter that we established for both strains (Figure S2A). We validated this method of normalization as outlined in Experimental Procedures and in Figures S2B and S2C. Our approach enabled us to determine that in the *rel*$^{-}$ strain transcript levels are globally increased relative to wild-type (Figure 2A), with approximately 67% of genes expressed at least 3-fold higher in the *rel*$^{-}$ strain than in wild-type at subjective dawn and 52% of genes expressed in this manner at subjective dusk (the term "subjective" refers to an internal estimate of time in constant light conditions). Functional analysis of genes overexpressed in the *rel*$^{-}$ strain reveals that they are enriched in genes encoding proteins involved in translation (Table S1 and Figure S2D). Our results suggest that the basal level of ppGpp is crucial for global control of transcription levels in unstressed conditions. Induction of ppGpp production in wild-type cyanobacterial cultures expressing an inducible version of the *E. coli* ppGpp synthetase RelA^{+} (Figure S3A) leads to subtle yet statistically significant suppression of gene expression in constant light relative to the control (in which an inactive version of RelA, RelA^{E335Q}, was expressed) at both time points we tested ($p < 0.0001$, as assessed by a paired t test) (Figures S3B and S3C). These results suggest that ppGpp acts to repress gene expression and that small changes in ppGpp levels during balanced growth in light globally affect gene expression in *S. elongatus*.

To test further the model that the basal level of ppGpp may be required to regulate global transcription rate during balanced growth in light, we compared global rates of RNA synthesis per cell in light in wild-type and in the *rel*$^{-}$ strain by [5,6-^{3}H]-uracil incorporation. We find that the global transcription rate per cell is higher in the *rel*$^{-}$ strain than in wild-type (Figure 2B), as are total RNA levels per cell (Figure 2C) and 16S and 23S rRNA levels (Figure S3E). Altogether, our results indicate that loss of *rel* leads to a global transcriptional increase, revealing the key role of basal levels of ppGpp in repressing transcription during growth in the absence of stress.

In bacteria, mRNA and protein synthesis are often tightly coupled (McGary and Nudler, 2013). Because we observed a globally increased transcription rate in the *rel*$^{-}$ strain that is associated with overexpression of genes involved in translation, as well as rRNA molecules, we hypothesized that translation may also be deregulated in the *rel*$^{-}$ cells. To test this idea, we measured global translation rate per cell using ^{35}S-methionine incorporation. We find that translation rate per cell is higher in the *rel*$^{-}$ strain than in wild-type (Figure 2D). We also observe that protein content per cell is higher in the *rel*$^{-}$ strain than in wild-type (Figure 2E) and that the mean length, mean width, and mean volume of *rel*$^{-}$ cells are larger than for wild-type cells (Figure 2F; Figure S3G), explaining the lower number of cells per OD_{750} in the *rel*$^{-}$ strain than in wild-type (Figure S2A). Furthermore, the *rel*^{D297A} synthetase-inactive mutant shows the same defect in cell size as the *rel*$^{-}$ mutant (Figure S3H). These results strongly suggest that translation and cell size regulation are aberrant in the (p)ppGpp-deficient strains. Finally, the *rel*$^{-}$ cells grow somewhat slower than wild-type under two light intensities (Figures S3I and S3J), suggesting that the basal level of ppGpp contributes to maintenance of optimal cell fitness during balanced growth.

Synthetic Restoration of Basal ppGpp Levels Rescues the Defects of the *rel*$^{-}$ Strain in Light

To determine whether the low concentration of ppGpp present during growth in light is sufficient to restore appropriate regulation of biosynthetic processes in the absence of *rel*, we asked which phenotypes of the *rel*$^{-}$ strain could be corrected by low-level expression of a constitutively active allele of *E. coli relA* (*relA*$^{+}$) in the *rel*$^{-}$ background (Figure 3A, top). We first compared levels of ppGpp in constant light in wild-type, the *rel*$^{-}$ + *relA*$^{+}$ strain, and the negative control, the RelA synthetase-deficient strain *rel*$^{-}$ + *relA*^{E335Q}. We find that ppGpp is produced in the *rel*$^{-}$ + *relA*$^{+}$ strain at a concentration comparable to that in wild-type (Figure 3A, bottom). Unlike in wild-type, however, pppGpp is not detected above background levels in the *rel*$^{-}$ + *relA*$^{+}$ strain (Figure S4A). The low concentration of ppGpp in the *rel*$^{-}$ + *relA*$^{+}$ strain is sufficient to globally lower gene expression levels, restoring a gene expression program similar to wild-type (Figure 3B; Figure S4C and S4D). By contrast, the negative control *rel*$^{-}$ + *relA*^{E335Q} strain has a transcriptional increase similar to that of the *rel*$^{-}$ strain (Figure S4C). Our findings indicate that the basal level of ppGpp is both necessary and sufficient to ensure a balanced transcriptional program in the cell during growth without stress.

To determine whether restoration of basal ppGpp levels corrects the size increase of the *rel*$^{-}$ strain, we analyzed the dimensions of the *rel*$^{-}$ + *relA*$^{+}$ cells, the *rel*$^{-}$ + *relA*^{E335Q} cells, wild-type, and the *rel*$^{-}$ cells. We find that low levels of ppGpp in the *rel*$^{-}$ + *relA*$^{+}$ strain are sufficient to significantly reduce cell dimensions of that strain (Figure 3C; Figure S4E) and that at lower OD_{750} values, the *rel*$^{-}$ + *relA*$^{+}$ strain grows as well as wild-type and better than the *rel*$^{-}$ strain at higher OD_{750} values (Figure S4F). Altogether, our results strongly support the idea that low levels of ppGpp are crucial for regulation of key aspects of cyanobacterial physiology and maintenance of cellular homeostasis during unstressed growth.

ppGpp Is Required for Correct Execution of Transcriptional Changes in Response to Darkness

Having established the key role of basal level of ppGpp for cell physiology during balanced growth, we next wanted to gain insight into the role of ppGpp signaling in stress tolerance during

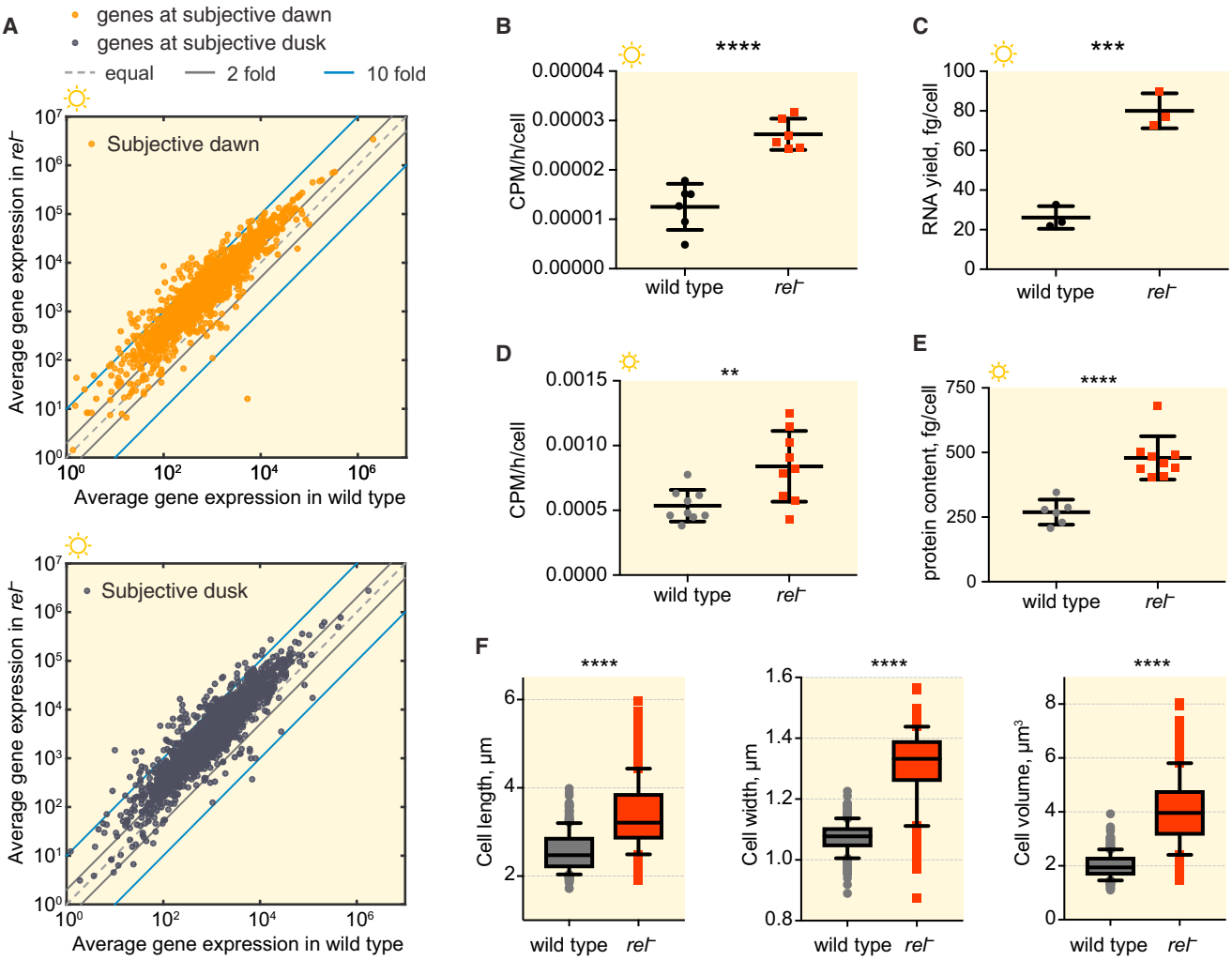

Figure 2. Characterization of the *rel*⁻ Mutant in Unstressed Conditions in Constant Light

(A) Comparison of the normalized average gene expression in wild-type and the *rel*⁻ strain at subjective dawn (top) and at subjective dusk (below) measured by RNA sequencing performed with exogenous RNA standards for normalization of read counts between the samples. Each point represents the mean expression value of two biological replicates. Fold changes are displayed graphically as diagonal lines on the plot.

(B) Comparison of global RNA synthesis rate per cell in wild-type and the *rel*⁻ strain measured by ^{3}H-uracil incorporation. Each point represents an individual measurement, and the mean and the SEM are indicated. Samples were statistically analyzed using the unpaired t test (****$p < 0.0001$). To verify our approach, we assessed global rates of RNA synthesis in wild-type cultures in the absence and in the presence of transcription inhibitor rifampicin (Figure S3D).

(C) Quantification of RNA content per cell in wild-type and the *rel*⁻ strain. Points represent individual measurements, and the mean and the SEM are indicated graphically. Data were statistically analyzed using the unpaired t test (***$p < 0.001$).

(D) Global translation rate per cell in wild-type and the *rel*⁻ strain determined by ^{35}S-methionine incorporation. Points represent individual measurements, and the mean and the SEM are indicated graphically. The unpaired t test was performed to analyze the data statistically, and **$p < 0.01$ ($p = 0.0078$). To verify our approach, we assessed global rates of protein synthesis in wild-type cultures in the absence and in the presence of translation inhibitor chloramphenicol (Figure S3F).

(E) Quantification of the total protein content per cell in wild-type and the *rel*⁻ strain. Each point represents a measurement performed in a biological replicate, and the mean and the SEM are indicated graphically. Data were statistically assessed using the unpaired t test (****$p < 0.0001$).

(F) Comparison of cell geometry measurements in wild-type and the *rel*⁻ cells. Cell length and width were obtained from microscopy images of 340 cells for each strain, and cell volume was calculated as described in Experimental Procedures. Center lines represent median values, box limits indicate the 25th and 75th percentiles, and whiskers extend from the 5th to the 95th percentile. Data were statistically analyzed using the unequal variance t test (****$p < 0.0001$).

See also Figures S2 and S3 and Table S1.

darkness. As reported by Hood et al. (2016), the *rel*⁻ strain is unable to grow in alternating light/dark conditions (Figure 4A) and exhibits a loss of viability during incubation in the dark (Figure S5A), suggesting that these defects are specifically triggered by exposure to darkness. Complementation of the *rel*⁻ strain with *rel* expressed from an ectopic site in the genome fully restores viability, while complementation with synthetase-deficient *rel*^{D297A} variant does not (Figure S5B), further indicating that ability to synthesize ppGpp is strictly required in cells to survive exposure to darkness.

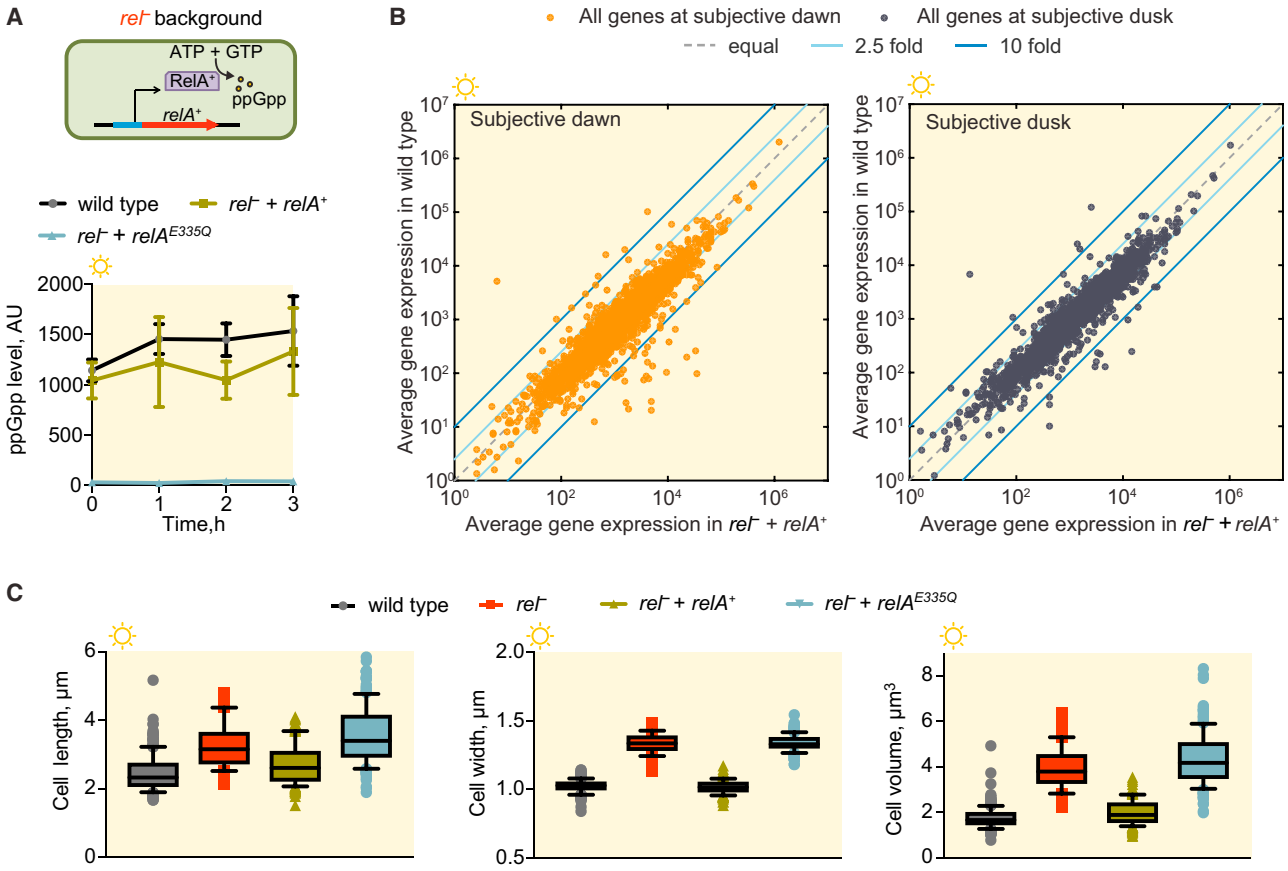

Figure 3. Effect of Restoration of the Basal ppGpp Level in the *rel*⁻ Strain on Transcription and Cell Size

(A) ppGpp levels in constant light conditions in the *rel*⁻ + *relA*⁺ strain (shown on the schematic diagram), the *rel*⁻ + *relA*^{E335Q} strain, and in wild-type. Points represent the mean of two experiments, with error bars displaying the SEM.

(B) Scatterplots comparing gene expression levels between wild-type and the *rel*⁻ + *relA*⁺ strain at subjective dawn and at subjective dusk. Points represent mean expression values for all genes obtained in two biological replicates. Equal expression and the cutoffs for 2.5-fold and 10-fold expression changes are indicated graphically with diagonal lines. The data were normalized using exogenous RNA standards, factoring in the number of cells harvested for RNA extraction (the relationship between OD_{750} and cell number per milliliter that we established for the *rel*⁻ + *relA*⁺ and the *rel*⁻ + *relA*^{E335Q} strains is presented in Figure S4B). Results of the functional analysis of genes substantially deregulated in the *rel*⁻ + *relA*⁺ strain (67 genes overexpressed at dawn, 34 genes overexpressed at dusk, 13 genes underexpressed at dawn, and 12 genes underexpressed at dusk) are provided in Table S2.

(C) Comparison of cell geometry measurements in wild-type, the *rel*⁻ cells, and the *rel*⁻ + *relA*⁺ and the *rel*⁻ + *relA*^{E335Q} strains. Cell length and width were obtained from microscopy images of 180 cells for each strain, and cell volume was calculated as described in Experimental Procedures. Center lines represent median values, box limits indicate the 25th and 75th percentiles, and whiskers extend from the 5th to the 95th percentile.

See also Figure S4 and Table S2.

When wild-type *S. elongatus* cells are transferred from light to dark conditions, the expression of most genes is rapidly repressed—transcription of more than 90% of genes is downregulated in darkness (Ito et al., 2009; Hosokawa et al., 2011). This dark-induced, genome-wide transcriptional shutdown has been proposed to be an active process that enables cells to reduce usage of ATP under nocturnal energy-limiting conditions (Takano et al., 2015), yet its underlying mechanism has not been elucidated. To understand whether ppGpp plays a role in the dark-induced transcriptional shutdown, we performed RNA sequencing analysis of the *rel*⁻ mutant strain and wild-type exposed to darkness at dusk for 12 hr. As in constant light, we find that in the dark, transcript levels are globally increased in the *rel*⁻ strain in comparison to wild-type (Figure 4B). To compare the dynamics of the transcriptional response to darkness in the *rel*⁻ strain and in wild-type, we normalized gene expression to the interval [0 1] separately for the *rel*⁻ strain and for wild-type. We observe that in wild-type, the dark-induced transcriptional shutdown is rapid and correlates with the dark-induced accumulation of high levels of ppGpp, with global repression of transcription occurring within 5 min of the onset of darkness. However, in the *rel*⁻ strain, the transcriptional shutdown is dysfunctional—it is significantly slower and happens to a lesser extent (Figure 4C). Toward the end of darkness, gene expression levels in the *rel*⁻ strain become closer to wild-type (Figure 4B, time point = 12 hr; Figure S5D), perhaps reflecting a passive restriction of transcription due to prolonged energy limitation or suggesting existence of another, slower ppGpp-independent mechanism to reduce gene

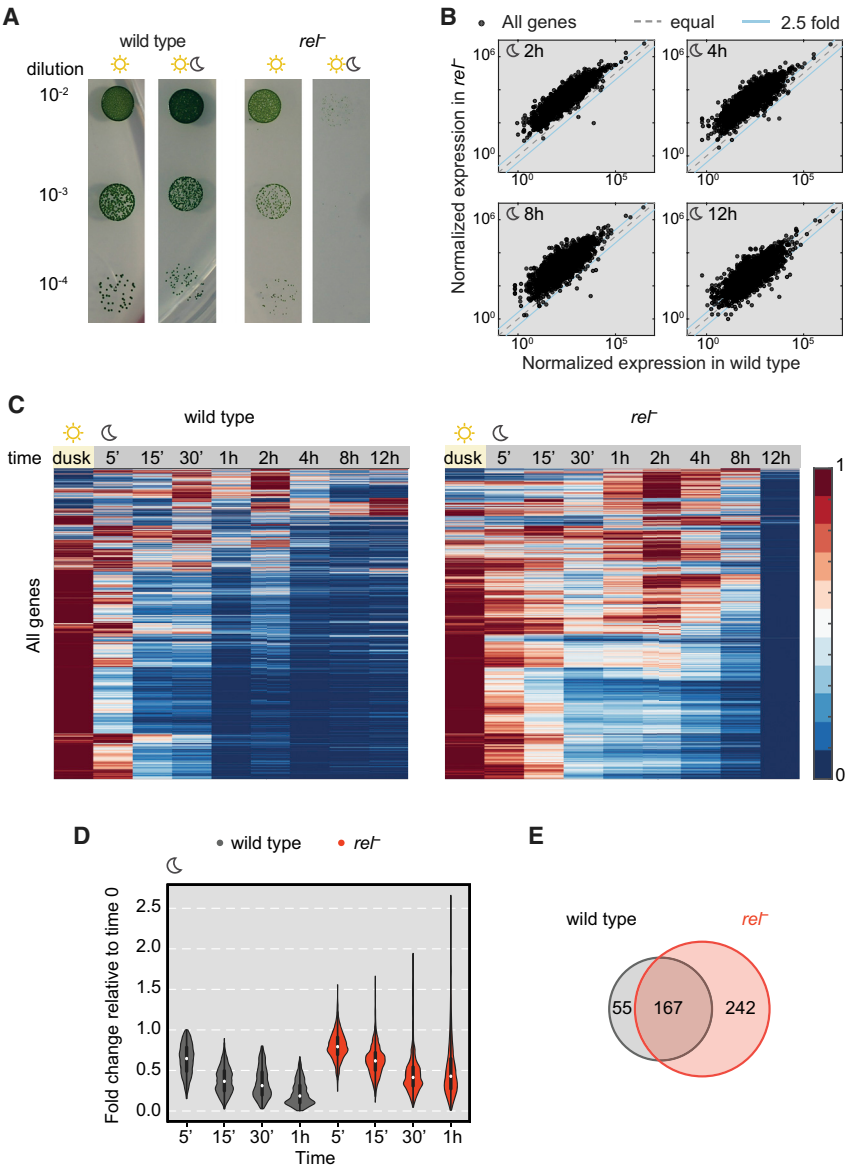

Figure 4. Effect of ppGpp on Transcription during Darkness

(A) Comparison of growth of wild-type and the *rel*⁻ strain using a plate-based assay. The experiment was performed three independent times, and a representative experiment is shown. Our results are in accordance with the viability experiment performed by Hood et al. (2016).

(B) Scatterplots comparing gene expression levels in wild-type and the *rel*⁻ mutant at four time points in the dark. Each point represents a mean expression value for each gene obtained using two biological replicates measured by RNA sequencing. Equal expression and the cutoffs for 2.5-fold expression changes are indicated graphically with diagonal lines.

(C) Heatmaps representing global gene expression in wild-type and the *rel*⁻ mutant at dusk and in darkness. Expression time courses of all genes were normalized to the interval [0 1] independently in each strain. Each row represents a gene, while columns represent normalized expression at an indicated time point. Genes in both heatmaps are displayed in the same order.

(D) Comparison of the dynamics of the dark-associated transcriptional shutdown in wild-type and the *rel*⁻ mutant. Violin plots represent distributions of fold change in expression of individual genes at indicated time points relative to their expression value at dusk. Values for 746 genes, whose expression is efficiently shut down in wild-type, are represented. White dots represent the medians of the distributions.

(E) Venn diagram representing the number of dark-induced genes in wild-type and the *rel*⁻ mutant. Dark-induced genes are defined as genes whose expression is at least 1.5 higher relative to its expression at dusk at a minimum two time points during exposure to darkness and whose average expression is higher than a threshold of 850 counts. A comparison of the number of dark-induced genes in wild-type detected by Ito et al. (2009) and in this study is presented in Figure S5C.

See also Figure S5 and Table S3.

expression in darkness. Further analysis of fold changes in expression of a group of 746 genes, highly expressed at dusk and rapidly repressed in the dark in wild-type, confirms that in the *rel*⁻ strain, the mechanism ensuring fast dark-induced transcriptional shutdown is compromised (Figure 4D). In wild-type, a small subset of genes is known to be induced under dark conditions (Hosokawa et al., 2011; Ito et al., 2009). We find that in the *rel*⁻ mutant, an additional 242 genes escape the shutdown and are expressed in response to darkness (Figure 4E; Table S3). Altogether, our findings strongly suggest that ppGpp signaling is required for an appropriate gene expression program in the dark and contributes to the rapid shutdown of transcriptional activity in response to darkness.

In many bacterial systems, (p)ppGpp is known to act by regulating transcription initiation through direct or indirect mechanisms affecting RNA polymerase (Barker et al., 2001; Krohn and Wagner, 1996; Liu et al., 2015). To elucidate whether the effects of ppGpp on transcription are associated with changes in RNA polymerase behavior on promoters, we performed RNA polymerase (RNAP) chromatin immunoprecipitation in the *rel*⁻ mutant and in wild-type cells exposed to dark. We analyzed the RNA polymerase pausing index, defined as the ratio between the maximum enrichment at the start of the transcription unit and the mean RNA polymerase enrichment within the gene body (Figure S5E). We observe that the RNA pausing index is globally higher in wild-type than in the *rel*⁻ strain at dusk and during darkness (Figure S5F). We also find that the fraction of transcription units with a proximally paused polymerase (defined as transcription units characterized by a RNA polymerase pausing index greater than 3) is higher in

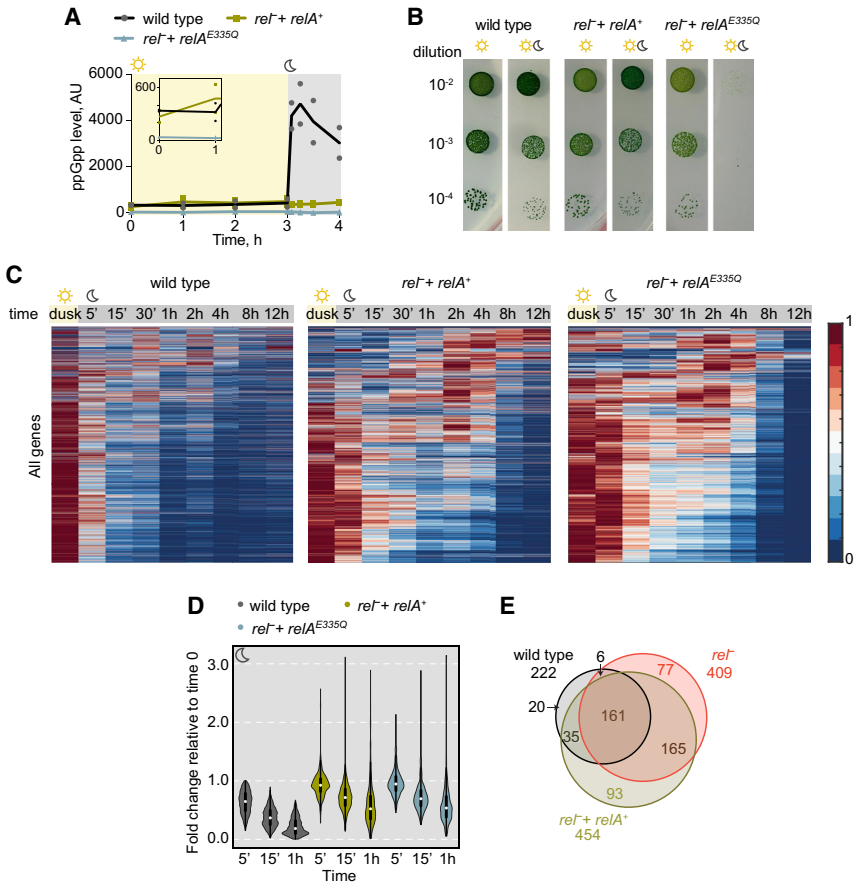

Figure 5. Effect of Restoration of Basal ppGpp Levels on Cell Viability and Transcriptional Regulation in the Dark

(A) ppGpp levels in light and after exposure to darkness in the *rel*⁻ + *relA*⁺ and the *rel*⁻ + *relA*^{E335Q} strains and in wild-type. Points represent individual measurements, and the lines represent the mean of two experiments. The inset shows a magnified view of ppGpp levels in light. Quantification of pppGpp levels is presented in Figure S6A.

(B) Comparison of growth of wild-type and the *rel*⁻ + *relA*⁺ and the *rel*⁻ + *relA*^{E335Q} strains in constant light and in light/dark conditions using a plate-based assay. The experiment was performed three independent times, and a representative experiment is shown.

(C) Heatmaps representing global gene expression in wild-type and the *rel*⁻ + *relA*⁺ and the *rel*⁻ + *relA*^{E335Q} strains at dusk and in darkness. Expression time courses of all genes were normalized to the interval [0 1] independently in each strain. The heatmap for wild-type was created by reordering data from Figure 4C so that genes in all three heatmaps are displayed in the same order. Each row represents a gene, while columns represent normalized expression at an indicated time point.

(D) Comparison of the dynamics of the transcriptional shutdown in wild-type and the *rel*⁻ + *relA*⁺ and the *rel*⁻ + *relA*^{E335Q} strains. Data representing the changes in wild-type are reproduced from Figure 4D to facilitate comparison. Medians of the distributions are displayed graphically as white points. As in Figure 4D, represented values correspond to changes in expression in 746 genes, whose expression is shut down in wild-type.

(E) Venn diagram representing the overlap of dark-induced genes in the *rel*⁻ + *relA*⁺ strain, wild-type, and the *rel*⁻ mutant.

See also Figure S6 and Table S4.

wild-type than the *rel*⁻ strain, with the exception of time points harvested at dawn after re-exposure to light (Figure S5G). These trends suggest that similar to other bacterial species, in cyanobacteria, ppGpp acts by globally affecting the behavior of RNA polymerase at promoters.

Basal Levels of ppGpp Are Sufficient for Survival of Darkness but Do Not Restore Dark-Induced Transcriptional Shutdown

To dissect the role of the basal ppGpp level versus ppGpp accumulation in regulation of adaptation to darkness, we confirmed that the *rel*⁻ + *relA*⁺ strain does not accumulate ppGpp in the dark (Figure 5A) and then asked whether the basal level of ppGpp is sufficient to protect the viability of cells grown in light/dark conditions. Surprisingly, we find that the *rel*⁻ + *relA*⁺ strain, despite its inability to induce ppGpp in response to darkness, can survive light/dark cycles (Figure 5B). Analysis of cell viability in prolonged darkness confirmed that the *rel*⁻ + *relA*⁺ strain persists these conditions almost as well as wild-type (Figure S6B). Thus, we conclude that the basal level of ppGpp is sufficient to protect cell viability in light/dark conditions.

To gain insight into the role of the basal level of ppGpp in the transcriptional response to darkness, we performed RNA sequencing on the *rel*⁻ + *relA*⁺ strain grown in light/dark conditions during exposure to darkness for 12 hr. In agreement with the results obtained in the *rel*⁻ + *relA*⁺ strain in constant light, we find that at dusk, transcript levels in this strain are more similar to wild-type levels (Figure S6C). However, when we normalized gene expression to the interval [0 1] separately for the *rel*⁻ + *relA*⁺ strain and the *rel*⁻ + *relA*^{E335Q} strain, we observed little difference in the dynamics of the shutdown between these strains (Figure 5C), indicating that the basal level of ppGpp is not sufficient to enable the dark-induced transcriptional shutdown. Further analysis of genes efficiently repressed in wild-type confirms that both the *rel*⁻ + *relA*⁺ and the *rel*⁻ + *relA*^{E335Q} strains are dysfunctional in their ability to rapidly shut down gene expression in response to darkness (Figure 5D). In agreement with this result, we find that a greater number of genes are dark induced in the *rel*⁻ + *relA*⁺ strain than in wild-type (Figure 5E; Table S4). Altogether, our results indicate that in light/dark cycles, low concentration of ppGpp is sufficient to prevent the global transcriptional increase characteristic of the *rel*⁻ strain; however, elevated levels of ppGpp in the dark are necessary for the appropriate execution of the rapid, dark-induced shutdown of transcription.

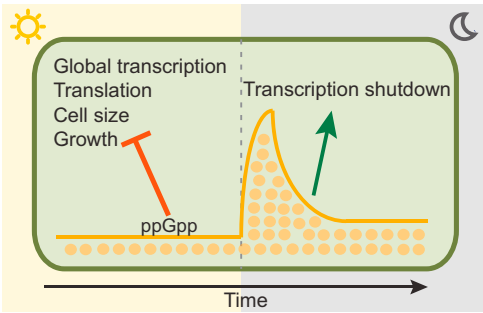

Figure 6. Model Representing the Physiological Role of (p)ppGpp in *S. elongatus* PCC7942 in Light and in Response to Darkness

DISCUSSION

Cyanobacteria use light as their energy source and face recurrent periods of energy limitation in darkness (Smith, 1983). A study by Hood et al. (2016) investigated the role of the stringent response in adaptation of cyanobacteria to darkness and showed that ppGpp accumulates in cyanobacteria in response to light deprivation. The authors proposed that elevated ppGpp levels are required to protect cell viability in the dark. Here, we show that (p)ppGpp signaling coordinates cyanobacterial metabolic balance both in constant light and in response to darkness (Figure 6). We propose a model in which the basal (p)ppGpp concentration profoundly affects global gene expression, translation, cell size, and growth in light, highlighting the critical contribution of low ppGpp levels to the control of normal cell physiology in unstressed conditions. Surprisingly, we find that basal levels of ppGpp are sufficient for viability in light/dark cycles, suggesting that the dramatic accumulation of (p)ppGpp observed in wild-type exposed to darkness is dispensable for survival of periods of energy limitation. In our model, viability of cyanobacterial cells in the dark depends on appropriate regulation of global transcription by basal levels of ppGpp. Although the elevated levels of the (p)ppGpp alarmones contribute to the dark-induced transcriptional shutdown, the ability to execute it is not essential under the conditions we tested in the laboratory. It is, however, possible that when complex stress stimuli occur simultaneously in nature, the accumulation of alarmones contributes to stress adaptation.

The stringent response was classically viewed as a cellular switch that elicits reorganization of gene expression programs in response to abiotic stresses. However, there has been a growing understanding that (p)ppGpp signaling functions as a molecular rheostat across a spectrum of environmental conditions, ranging from nutrient rich to nutrient poor (Traxler et al., 2011; Balsalobre, 2011; Gaca et al., 2013, 2015) and allowing cells to adjust their transcriptional program to environmental constraints. Increasing (p)ppGpp levels in *E. coli* are inversely correlated with growth rate (Sokawa et al., 1975; Ryals et al., 1982; Sarubbi et al., 1988; Potrykus et al., 2011). Furthermore, it has been determined that different levels of starvation activate stringent response in *E. coli* to a different extent (Traxler et al., 2011). The responsiveness of *S. elongatus* cells to both very low and high (p)ppGpp concentrations is consistent with this molecular rheostat model, indicating that (p)ppGpp-mediated concentration-dependent regulation of metabolic balance may be a conserved regulatory feature across the bacterial world. Coupling alarmone production to the activity of the photosynthetic electron transport chain may allow cyanobacteria to efficiently fine-tune their internal metabolic balance with fluctuations in light conditions. How this photosynthesis-dependent regulation of Rel is achieved on a molecular level remains to be investigated. Given the rapidity of (p)ppGpp accumulation on exposure to darkness, we expect that this regulation is based on post-translational mechanisms.

Our work provides insight into transcriptional profiles of the ppGpp-deficient strain and uncovers previously unnoticed global transcriptional increase in these cells. This transcriptional increase may be a feature shared across all bacteria devoid of (p)ppGpp, overlooked due to the nature of standard approaches used in gene expression studies. It will be interesting to revisit global expression changes during stringent response in other systems using quantitative techniques such as the one applied here. The molecular mechanism underlying transcription regulation by (p)ppGpp in cyanobacteria is unknown, and further studies are required to unravel it.

Finally, ppGpp and the enzymes responsible for its metabolism have been detected in green algae and plants (van der Biezen et al., 2000; Takahashi et al., 2004; Atkinson et al., 2011). ppGpp accumulates in chloroplasts following exposure to environmental stresses such as wounding, pathogens, heat shock, or drought (Takahashi et al., 2004), suggesting that the stringent response-like signaling may participate in adaptation of plants to adverse conditions. Changing basal (p)ppGpp concentration through overexpression of one of the Rel/SpoT homolog enzymes in *Arabidopsis thaliana* results in reduction of chloroplast size and alters transcript levels in chloroplasts (Maekawa et al., 2015; Sugliani et al., 2016), which is in accord with our observations in *S. elongatus*. It is, thus, possible that (p)ppGpp-mediated homeostatic control plays an important role in unstressed conditions in all photoautotrophs, perhaps affecting their productivity, biomass, and growth. Further work is required to fully understand the implications of (p)ppGpp signaling in photosynthesizing organisms.

EXPERIMENTAL PROCEDURES

Cyanobacterial Strains

Wild-type *S. elongatus* PCC7942 was obtained from the American Type Culture Collection. All strains used in this study are listed in Table S5. Details of strain construction are provided in Supplemental Experimental Procedures.

Cell Culture

Cell cultures of wild-type and mutant cells were grown in BG-11 medium at 30°C under illumination with cool fluorescent light at 40 μE m^{-2} s^{-1} (micromoles of photons per square meters per second) unless indicated otherwise in figure legends. Strains for all experiments were entrained by exposure to 12 hr of darkness, followed by 12 hr of light, followed by another 12 hr of darkness. In experiments involving dark treatment, cultures were exposed to darkness in phase with their entrainment cycle. In the experiments presented in Figures S3A–S3C, cells were induced with 1.6 mM theophylline at subjective dusk (circadian time = 12 hr).

Growth and Viability Assays

Growth and viability assays were performed as described in Puszynska and O'Shea (2017) and are detailed in Supplemental Experimental Procedures.

Formic Acid Extraction and Chromatography

Separation and quantitation of (p)ppGpp were performed following Cashel (1969) with modifications. Briefly, entrained cultures were treated with 100 μCi/mL of ^{32}P-orthophosphoric acid (PerkinElmer) 24 hr before the start of cell sampling. Aliquots of cultures were mixed with one-half volume of 98% formic acid, incubated on ice for 20 min, and clarified by centrifugation at 3,000 × *g* for 10 min at 4°C. The supernatant was collected and frozen overnight at −20°C. Samples were then thawed, and 10 μL aliquots were spotted on polyethylenimine (PEI)-cellulose thin chromatography glass plates (EMD Millipore). The plates were developed in chromatographic chambers containing 100–150 mL of 1.5 M KH_2PO_4 (pH 3.4) until the solvent front reached approximately 17 cm above the origin. The thin-layer chromatography (TLC) plates were dried and exposed to phosphorimaging plates for 8 hr, which were then scanned using a Typhoon Imaging System (GE Healthcare Life Sciences). ImageJ (Schindelin et al., 2015) was used to quantify the levels of (p)ppGpp. The nucleotides migrated in the expected R_f ranges. In addition, identification of guanosine triphosphate (GTP) was verified by comparison with migration of γ-^{32}P GTP (PerkinElmer).

Protein Separation and Immunoblotting

To analyze expression of RelA^{+} and RelA^{E335Q}, cells were induced with 1.6 mM theophylline, harvested for immunoblotting by filtration, and frozen in liquid nitrogen. Cells were resuspended in ice-cold lysis buffer (8 M urea, 20 mM HEPES [pH 8.0], and 1 mM β-mercaptoethanol) and disrupted by bead beating with 0.1 mm glass beads for total of 5 min, with periodic cooling on ice. Cell lysates were clarified by centrifugation. Protein concentration of each sample was determined by Bradford assay (Bio-Rad). Cell lysates were loaded on 4%–20% Tris-Glycine Gel (Novex). Proteins were transferred to a nitrocellulose membrane using a semi-dry transfer apparatus (Bio-Rad). The membrane was blocked in tris-buffered saline, 0.1% tween 20 (TBST) + 2.5% milk and then incubated with a monoclonal anti-FLAG M2 mouse antibody (Sigma-Aldrich). Quantification of the immunoblots was performed using ImageJ software.

Estimation of Cell Number

Cells were counted using the Beckman Coulter Multisizer III fitted with a 30 μm aperture tube. 10 μL aliquots of cultures varying in OD_{750} were thoroughly mixed with 10 mL of the Isoton II diluent, and 100 μL of the cell suspensions were sampled by the instrument. At least two replicate measurements were performed per culture, and the mean was taken as the representative cell count. Linear regression analysis was performed to establish the relationship between OD_{750} and cell number per milliliter for all analyzed strains.

Protein Content per Cell

To quantify total protein content per cell in wild-type and the *rel*$^{-}$ strain, 10 mL of cultures at a range of OD_{750} were harvested by filtration. Cells were resuspended in 300 μL ice-cold urea lysis buffer (8 M urea, 20 mM HEPES [pH 8.0], and 1 mM β-mercaptoethanol) and disrupted by bead beating. Whole-cell lysates were clarified by centrifugation. The total amount of protein in the lysates was determined using the Bradford assay (Bio-Rad) with a standard curve prepared with BSA (Pierce). The total protein content per cell was estimated by counting cells before lysis using the Beckman Coulter Multisizer III and dividing the amount of the protein in the given lysate by the cell number used to prepare the lysate.

Preparation of Exogenous RNA Standards

The strategy for preparation of RNA standards for RNA sequencing is based on Gifford et al. (2011) and Satinsky et al. (2013). Five genes (*bub2*, *mam1*, *pcl9*, *uba3*, and *nyv1*) from *Saccharomyces cerevisiae* were selected as RNA standards, ensuring they bear no identity to the *S. elongatus* PCC7942 genome. Sequences of the standards are provided in Supplemental Experimental Procedures. The standards were PCR amplified using Phusion High-Fidelity DNA Polymerase (NEB) with primers containing a T7 promoter sequence at the 5′ end of the forward primer. The list of primers is provided in Supplemental Experimental Procedures. The PCR products were purified using a QIAquick PCR purification kit (QIAGEN), and aliquots of each PCR product were run on the DNA High Sensitivity Chip (Agilent) to verify that a single fragment of expected length was produced. *In vitro* transcription of RNA standards was performed using the MEGAscript High Yield Transcription Kit (Ambion), with the PCR amplicons as templates. The synthesized RNA standards were purified using the MegaClear Transcription Clean-Up Kit (Ambion) and quantified using the Quant-iT RiboGreen RNA Assay Kit (Invitrogen). To verify that a single RNA species was produced in each reaction, Agilent RNA Nano Chip was run. The standards were then aliquoted and kept at −80°C.

RNA Isolation

Total RNA isolation was performed by the hot phenol method. Strains were entrained, and 10 mL of cultures were harvested by filtering at indicated time points and frozen in liquid nitrogen. Before cell resuspension. RNA standards were added to the AE buffer (50 mM CH_3COONa [pH 5.2] and 10 mM EDTA) and thoroughly mixed. Cells were resuspended in 12 mL of the AE buffer and transferred to phenol-resistant tubes containing 1 mL of 20% SDS. 12 mL of unbuffered acid phenol was added to each tube. Tubes were incubated for 10 min at 65°C with continuous vortexing, chilled on ice for 5 min, and centrifuged for 30 min at 17,000 × *g* at 4°C. The supernatant was transferred to a new phenol-resistant tube, and 1 mL of 3 M CH_3COONa (pH 5.2) and 10 mL of isopropanol were added. Following overnight precipitation at −20°C, extracts were centrifuged for 30 min at 17,000 × *g* at 4°C, and the pellets were washed with 70% ethanol, air-dried, and resuspended in nuclease-free water. Following DNA digestion with RQ1 RNase Free DNase (Promega), standard phenol-chloroform extraction was performed. RNA integrity was assessed on an agarose gel.

For comparison of total RNA content in wild-type and the *rel*$^{-}$ cells, no exogenous RNA standards were added to the AE buffer. RNA content was calculated by dividing the total yield of RNA by the number of cells used to perform the extraction.

RNA Sequencing

Ribosomal RNA depletion was performed using the Ribo-Zero rRNA Removal Gram-Negative Bacteria Kit (Illumina). Strand-specific RNA sequencing libraries were prepared using the TruSeq Stranded mRNA Sample Prep Kit (Illumina). Samples were sequenced on an Illumina HiSeq machine by the Bauer Core Facility at Harvard University. Sequences were aligned to the genome as in Puszynska and O'Shea (2017). To quantify gene expression, we counted the number of coding reads between the start and the stop positions of open reading frames. Normalization was performed using the exogenous RNA standards and cell number (Table S6), except for Figures S3B and S3C, in which we used reads per million (RPM) normalization. We validated our approach by comparing gene expression changes at subjective dawn and subjective dusk in wild-type using either RPM normalization or normalization with exogenous RNA standards (Figure S2B), observing that these methods produce similar results when global changes in mRNA levels are not expected to occur. We also selected five genes for qRT-PCR validation and observed fold changes in expression in the *rel*$^{-}$ strain relative to wild-type, consistent with results obtained by RNA sequencing followed by normalization with exogenous RNA standards (Figure S2C).

Analyses of the functional annotation clusters of the protein coding genes were performed using Database for Annotation, Visualization, and Integrated Discovery (DAVID) Bioinformatics Resources.

qRT-PCR for Gene Expression and rRNA Quantitation

qRT-PCR was carried out using SYBR Green PCR Master Mix (Applied Biosystems), SuperScript III Reverse Transcriptase (Invitrogen), and the primers listed in Supplemental Experimental Procedures. The abundance of transcripts was normalized by an RNA standard *bub2* (16S rRNA and 23S rRNA quantitation in *rel*$^{-}$ relative to wild-type) (Figure S3E) or *uba3* (Figure S2C) from *S. cerevisiae* added to the RNA AE extraction buffer and extracted, together with *S. elongatus* RNA.

Chromatin Immunoprecipitation and ChIP-Seq

Chromatin immunoprecipitation was performed following Vijayan et al. (2011) and Markson et al. (2013) with modifications. Details are provided in Supplemental Experimental Procedures.

Cell Size Analysis

Cells grown to mid-log phase were placed under BG-11 agar pads, and images were acquired by capturing the cells' red autofluorescence using a Zeiss Axiovert 200M inverted microscope equipped with a Yokogawa CSU-10 spinning disc, a Cascade 512B EM-CCD camera (Photometrics), a 561 nm laser (Coherent), a Plan-Apochromat 100×/1.40 Oil Ph3 objective (Zeiss), and Metamorph 7.8.8 acquisition software (Molecular Devices). Cell length and width analyses were performed in Fiji software (Schindelin et al., 2012) using the MicrobeJ plug-in (Ducret et al., 2016). Cell volume (V) was approximated from the cell length (l) and cell width (w) by assuming the cell is a cylinder capped with two hemispheres, using a formula $V = \pi^{*}w^{2*}(l - w/3)/4$ (Volkmer and Heinemann, 2011). Data were statistically evaluated using Welch's unequal variances t test in GraphPad Prism 7.0.

Global Transcription Rate Analysis

To establish global RNA synthesis rate, cells were labeled with 1.25 μCi/mL of [5,6-^{3}H] uracil for 30 min, harvested by centrifugation for 10 min at 3,000 × *g* at 4°C, and washed with ice-cold PBS. Pellets were extracted with ice-cold 5% trichloroacetic acid and 4 M urea for 20 min on ice. The suspension was collected on Whatman GF/C filters and washed twice with ice-cold 1% trichloroacetic acid (TCA) with 1 mM uracil. The filters were dried, and the incorporated radioactivity was counted using the Beckman Coulter LS6500 Liquid Scintillation Counter.

Global Translation Rate Analysis

To measure the global protein synthesis rate, cells were labeled with 2.5 μCi/mL of EasyTag L-[^{35}S]-methionine for either 20 or 30 min. Cells were harvested by centrifugation for 10 min at 3,000 × *g* at 4°C and washed with ice-cold PBS. Pellets were frozen until extraction in urea buffer (8 M urea, 20 mM HEPES [pH 8.0], and 1 mM β-mercaptoethanol) and disrupted by bead beating. Cell lysates were clarified by centrifugation. Aliquots of the lysates were spotted on P81 Whatman filters, air-dried in a laminar flow hood, and precipitated in ice-cold 5% TCA for 5 min. Filters were then washed twice with ice-cold 10% TCA, twice with 200-proof ethanol, and once with acetone and were air-dried in the laminar flow hood. The incorporated radioactivity was measured using the Beckman Coulter LS6500 Liquid Scintillation Counter.

In our work, we represent global transcription and translation rates in terms of the product made per unit time per cell representing total transcriptional and translational activity in the cell. An alternative measure of transcription and translation is rate normalized per volume, which relates to the rate of change of concentration of RNA or protein due to synthesis. Given the difference in cell size, the rate of transcription and translation per unit volume is not significantly different between the *rel*$^{-}$ strain and wild-type.

DATA AND SOFTWARE AVAILABILITY

The accession number for all datasets reported in this paper is GEO: GSE10360.

SUPPLEMENTAL INFORMATION

Supplemental Information includes Supplemental Experimental Procedures, six figures, and six tables and can be found with this article online at https://doi.org/10.1016/j.celrep.2017.11.067.

ACKNOWLEDGMENTS

We thank members of the O'Shea and Denic labs for technical assistance, constructive criticism, and comments on the manuscript. We thank Christian Daly from the Bauer Core Facility for performing sequencing runs. This work was funded by the Howard Hughes Medical Institute (CC30750).

AUTHOR CONTRIBUTIONS

A.M.P. and E.K.O. designed and wrote the paper. A.M.P. performed experiments and analyzed data.

DECLARATION OF INTERESTS

The authors declare no competing interests.

Received: October 17, 2017
Revised: November 10, 2017
Accepted: November 17, 2017
Published: December 12, 2017

REFERENCES

Atkinson, G.C., Tenson, T., and Hauryliuk, V. (2011). The RelA/SpoT homolog (RSH) superfamily: distribution and functional evolution of ppGpp synthetases and hydrolases across the tree of life. PLoS ONE *6*, e23479.

Balsalobre, C. (2011). Concentration matters!! ppGpp, from a whispering to a strident alarmone. Mol. Microbiol. *79*, 827–829.

Barker, M.M., Gaal, T., Josaitis, C.A., and Gourse, R.L. (2001). Mechanism of regulation of transcription initiation by ppGpp. I. Effects of ppGpp on transcription initiation *in vivo* and *in vitro*. J. Mol. Biol. *305*, 673–688.

Battesti, A., and Bouveret, E. (2006). Acyl carrier protein/SpoT interaction, the switch linking SpoT-dependent stress response to fatty acid metabolism. Mol. Microbiol. *62*, 1048–1063.

Boutte, C.C., and Crosson, S. (2013). Bacterial lifestyle shapes stringent response activation. Trends Microbiol. *21*, 174–180.

Cashel, M. (1969). The control of ribonucleic acid synthesis in *Escherichia coli*. IV. Relevance of unusual phosphorylated compounds from amino acid-starved stringent strains. J. Biol. Chem. *244*, 3133–3141.

Cashel, M., and Gallant, J. (1969). Two compounds implicated in the function of the RC gene of *Escherichia coli*. Nature *221*, 838–841.

Doolittle, W.F. (1979). The cyanobacterial genome, its expression, and the control of that expression. Adv. Microb. Physiol. *20*, 1–102.

Douglas, A.E., and Raven, J.A. (2003). Genomes at the interface between bacteria and organelles. Philos. Trans. R. Soc. Lond. B Biol. Sci. *358*, 5–17, discussion 517–518.

Ducret, A., Quardokus, E., and Brun, Y. (2016). MicrobeJ, a high throughput tool for quantitative bacterial cell detection and analysis. Nat. Microbiol. *1*, 16077.

Gaca, A.O., Kajfasz, J.K., Miller, J.H., Liu, K., Wang, J.D., Abranches, J., and Lemos, J.A. (2013). Basal levels of (p)ppGpp in *Enterococcus faecalis*: the magic beyond the stringent response. MBio *4*, e00646–13.

Gaca, A.O., Colomer-Winter, C., and Lemos, J.A. (2015). Many means to a common end: the intricacies of (p)ppGpp metabolism and its control of bacterial homeostasis. J. Bacteriol. *197*, 1146–1156.

Gifford, S.M., Sharma, S., Rinta-Kanto, J.M., and Moran, M.A. (2011). Quantitative analysis of a deeply sequenced marine microbial metatranscriptome. ISME J. *5*, 461–472.

Hauryliuk, V., Atkinson, G.C., Murakami, K.S., Tenson, T., and Gerdes, K. (2015). Recent functional insights into the role of (p)ppGpp in bacterial physiology. Nat. Rev. Microbiol. *13*, 298–309.

Hogg, T., Mechold, U., Malke, H., Cashel, M., and Hilgenfeld, R. (2004). Conformational antagonism between opposing active sites in a bifunctional RelA/SpoT homolog modulates (p)ppGpp metabolism during the stringent response [corrected]. Cell *117*, 57–68.

Hood, R.D., Higgins, S.A., Flamholz, A., Nichols, R.J., and Savage, D.F. (2016). The stringent response regulates adaptation to darkness in the cyanobacterium *Synechococcus elongatus*. Proc. Natl. Acad. Sci. USA *113*, E4867–E4876.

Hosokawa, N., Hatakeyama, T.S., Kojima, T., Kikuchi, Y., Ito, H., and Iwasaki, H. (2011). Circadian transcriptional regulation by the posttranslational oscillator without de novo clock gene expression in *Synechococcus*. Proc. Natl. Acad. Sci. USA *108*, 15396–15401.

Ito, H., Mutsuda, M., Murayama, Y., Tomita, J., Hosokawa, N., Terauchi, K., Sugita, C., Sugita, M., Kondo, T., and Iwasaki, H. (2009). Cyanobacterial daily life with Kai-based circadian and diurnal genome-wide transcriptional control in *Synechococcus elongatus*. Proc. Natl. Acad. Sci. USA *106*, 14168–14173.

Kamarthapu, V., Epshtein, V., Benjamin, B., Proshkin, S., Mironov, A., Cashel, M., and Nudler, E. (2016). ppGpp couples transcription to DNA repair in *E. coli*. Science *352*, 993–996.

Kanjee, U., Ogata, K., and Houry, W.A. (2012). Direct binding targets of the stringent response alarmone (p)ppGpp. Mol. Microbiol. *85*, 1029–1043.

Kriel, A., Bittner, A.N., Kim, S.H., Liu, K., Tehranchi, A.K., Zou, W.Y., Rendon, S., Chen, R., Tu, B.P., and Wang, J.D. (2012). Direct regulation of GTP homeostasis by (p)ppGpp: a critical component of viability and stress resistance. Mol. Cell *48*, 231–241.

Krohn, M., and Wagner, R. (1996). Transcriptional pausing of RNA polymerase in the presence of guanosine tetraphosphate depends on the promoter and gene sequence. J. Biol. Chem. *271*, 23884–23894.

Liu, K., Bittner, A.N., and Wang, J.D. (2015). Diversity in (p)ppGpp metabolism and effectors. Curr. Opin. Microbiol. *24*, 72–79.

Maekawa, M., Honoki, R., Ihara, Y., Sato, R., Oikawa, A., Kanno, Y., Ohta, H., Seo, M., Saito, K., and Masuda, S. (2015). Impact of the plastidial stringent response in plant growth and stress responses. Nat. Plants *1*, 15167.

Markson, J.S., Piechura, J.R., Puszynska, A.M., and O'Shea, E.K. (2013). Circadian control of global gene expression by the cyanobacterial master regulator RpaA. Cell *155*, 1396–1408.

McGary, K., and Nudler, E. (2013). RNA polymerase and the ribosome: the close relationship. Curr. Opin. Microbiol. *16*, 112–117.

Potrykus, K., and Cashel, M. (2008). (p)ppGpp: still magical? Annu. Rev. Microbiol. *62*, 35–51.

Potrykus, K., Murphy, H., Philippe, N., and Cashel, M. (2011). ppGpp is the major source of growth rate control in *E. coli*. Environ. Microbiol. *13*, 563–575.

Puszynska, A.M., and O'Shea, E.K. (2017). Switching of metabolic programs in response to light availability is an essential function of the cyanobacterial circadian output pathway. eLife *6*, e23210.

Ryals, J., Little, R., and Bremer, H. (1982). Control of rRNA and tRNA syntheses in *Escherichia coli* by guanosine tetraphosphate. J. Bacteriol. *151*, 1261–1268.

Sarubbi, E., Rudd, K.E., and Cashel, M. (1988). Basal ppGpp level adjustment shown by new *spoT* mutants affect steady state growth rates and *rrnA* ribosomal promoter regulation in *Escherichia coli*. Mol. Gen. Genet. *213*, 214–222.

Satinsky, B.M., Gifford, S.M., Crump, B.C., and Moran, M.A. (2013). Use of internal standards for quantitative metatranscriptome and metagenome analysis. Methods Enzymol *531*, 237–250.

Schindelin, J., Arganda-Carreras, I., Frise, E., Kaynig, V., Longair, M., Pietzsch, T., Preibisch, S., Rueden, C., Saalfeld, S., Schmid, B., et al. (2012). Fiji: an open-source platform for biological-image analysis. Nat. Methods *9*, 676–682.

Schindelin, J., Rueden, C.T., Hiner, M.C., and Eliceiri, K.W. (2015). The ImageJ ecosystem: an open platform for biomedical image analysis. Mol. Reprod. Dev. *82*, 518–529.

Smith, A.J. (1983). Modes of cyanobacterial carbon metabolism. Ann. Microbiol. (Paris) *134B*, 93–113.

Sokawa, Y., Sokawa, J., and Kaziro, Y. (1975). Regulation of stable RNA synthesis and ppGpp levels in growing cells of *Escherichia coli*. Cell *5*, 69–74.

Srivatsan, A., and Wang, J.D. (2008). Control of bacterial transcription, translation and replication by (p)ppGpp. Curr. Opin. Microbiol. *11*, 100–105.

Sugliani, M., Abdelkefi, H., Ke, H., Bouveret, E., Robaglia, C., Caffarri, S., and Field, B. (2016). An ancient bacterial signaling pathway regulates chloroplast function to influence growth and development in *Arabidopsis*. Plant Cell *28*, 661–679.

Surányi, G., Korcz, A., Pálfi, Z., and Borbély, G. (1987). Effects of light deprivation on RNA synthesis, accumulation of guanosine 3′(2′)-diphosphate 5′-diphosphate, and protein synthesis in heat-shocked *Synechococcus* sp. strain PCC 6301, a cyanobacterium. J. Bacteriol. *169*, 632–639.

Takahashi, K., Kasai, K., and Ochi, K. (2004). Identification of the bacterial alarmone guanosine 5′-diphosphate 3′-diphosphate (ppGpp) in plants. Proc. Natl. Acad. Sci. USA *101*, 4320–4324.

Takano, S., Tomita, J., Sonoike, K., and Iwasaki, H. (2015). The initiation of nocturnal dormancy in *Synechococcus* as an active process. BMC Biol. *13*, 36.

Traxler, M.F., Zacharia, V.M., Marquardt, S., Summers, S.M., Nguyen, H.-T., Stark, S.E., and Conway, T. (2011). Discretely calibrated regulatory loops controlled by ppGpp partition gene induction across the "feast to famine" gradient in *Escherichia coli*. Mol. Microbiol. *79*, 830–845.

van der Biezen, E.A., Sun, J., Coleman, M.J., Bibb, M.J., and Jones, J.D. (2000). *Arabidopsis* RelA/SpoT homologs implicate (p)ppGpp in plant signaling. Proc. Natl. Acad. Sci. USA *97*, 3747–3752.

Vijayan, V., Jain, I.H., and O'Shea, E.K. (2011). A high resolution map of a cyanobacterial transcriptome. Genome Biol. *12*, R47.

Volkmer, B., and Heinemann, M. (2011). Condition-dependent cell volume and concentration of *Escherichia coli* to facilitate data conversion for systems biology modeling. PLoS ONE *6*, e23126.

Cell Reports, Volume *21*

Supplemental Information

ppGpp Controls Global Gene Expression in Light and in Darkness in *S. elongatus*

Anna M. Puszynska and Erin K. O'Shea

Puszynska and O'Shea Figure S1

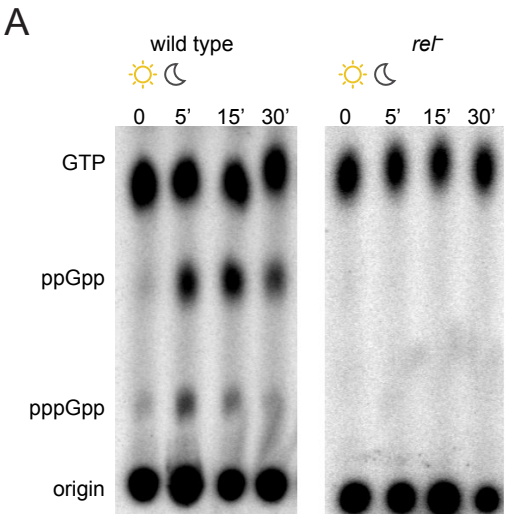

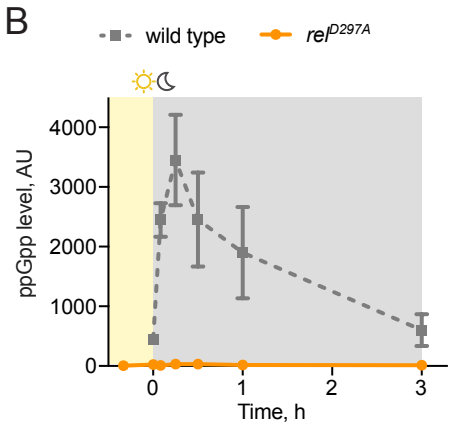

Figure S1. Influence of mutations in *rel* on (p)ppGpp accumulation. Related to Figure 1.
(A) Image of representative thin-layer chromatography plates displaying levels of indicated nucleotides in wild-type and the *rel*$^{-}$ strain in light and after exposure to darkness. Superfluous lanes and the upper part of the plates are not shown. (B) Quantitation of ppGpp levels in *rel*^{D297A} (*rel* variant lacking ppGpp synthase activity) in response to exposure to darkness. Data representing the ppGpp levels in wild-type are reproduced from Figure 1B to facilitate comparison.

Puszynska and O'Shea Figure S2

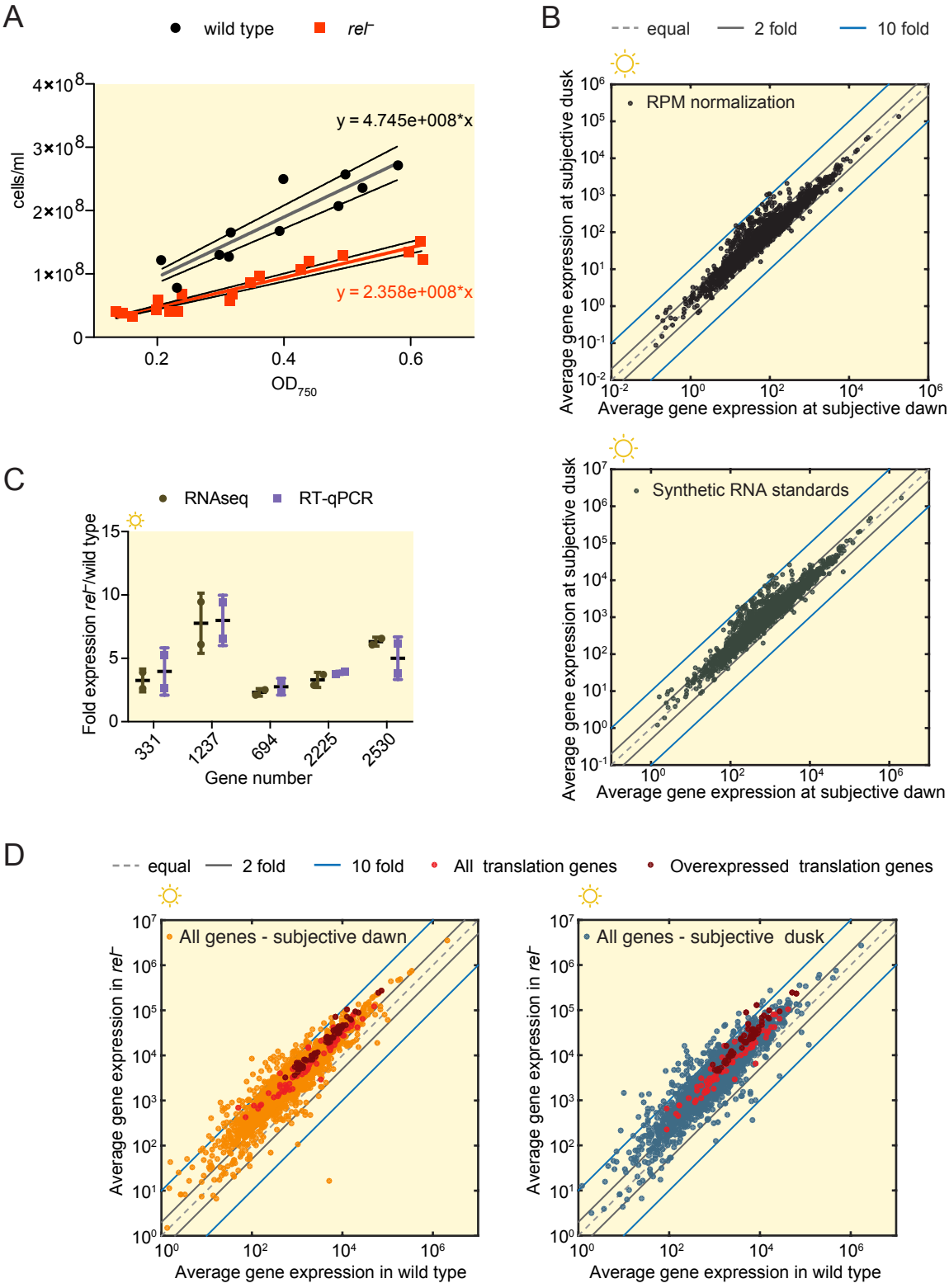

Figure S2. Analysis of transcriptional changes in the *rel*⁻ strain. Related to Figure 2

(A) Relationship between cell number per ml and OD_{750} for wild-type and the *rel*⁻ strain. Points represent individual measurements, while the gray and red lines correspond to the best fit lines obtained using linear regression analysis. The 95% confidence bands for each graph are shown using black lines. Equations describing the relationship between cell number per ml and OD_{750} for wild-type and the *rel*⁻ strain are represented in black and red respectively. (B) Scatter plots representing comparisons of mean gene expression values at subjective dawn and at subjective dusk in wild-type cells. Each point represents an average expression value for a gene obtained using either RPM normalization (top), or synthetic RNA standard normalization method (below). Fold changes are displayed graphically as diagonal lines on the plot. (C) Comparison of fold-change expression values for five genes in the *rel*⁻ strain relative to wild-type at subjective dusk assessed by RNA-seq and by RT-qPCR. Points represent individual measurements and the mean and the standard deviation are represented graphically. (D) Scatter plots representing gene expression levels in wild-type and the *rel*⁻ strain at subjective dawn (left) and at subjective dusk (right). Each point represents a mean expression value of two biological replicates. All translation genes are indicated in red, while translation genes meeting the criteria for genes highly overexpressed in the *rel*⁻ strain are represented in dark red (> 3.5-fold change in expression, and difference in normalized counts between the *rel*⁻ strain and wild-type > 1000). Fold changes are displayed graphically as diagonal lines on the plot.

Puszynska and O'Shea Figure S3

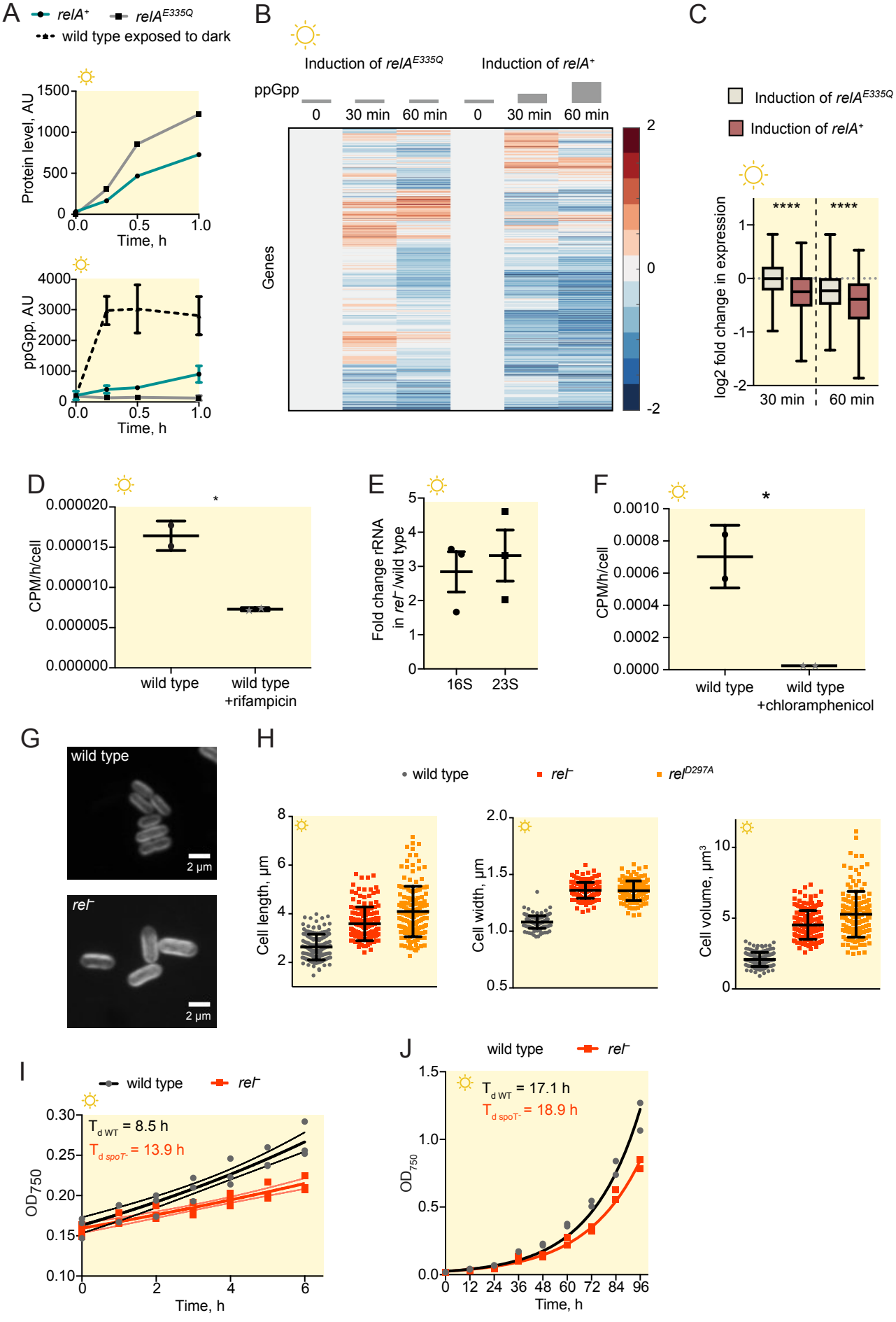

Figure S3 Characterization of ppGpp overproducing strain and the *rel*⁻ strain in light. Related to Figure 2.

(A) Quantitation of $RelA^{+}$ and $RelA^{E335Q}$ protein levels (left) and relative levels of ppGpp in the $relA^{+}$ and $relA^{E335Q}$ strains (right) following induction with 1.6 mM theophylline at time t = 0 (subjective dusk). Points represent the mean of two experiments with error bars displaying the standard error of the mean. (B) Heat map representing log2 transformed fold changes in global gene expression upon induction of either constitutively active RelA ($RelA^{+}$) or the inactive RelA mutant ($RelA^{E335Q}$) in cultures entrained by two light/dark cycles measured by RNA-seq. Rows represent all genes whose RPM-normalized mean expression value is above the cutoff of 50. Columns represent the log2 transformed fold change of expression of each gene relative to time 0 (CT = 12 h, subjective dusk). (C) Box plots comparing log2 transformed fold changes in global gene expression upon induction of either constitutively active RelA ($RelA^{+}$) or the inactive RelA mutant ($RelA^{E335Q}$) relative to time 0. All genes whose RPM-normalized mean expression value is above the cutoff of 50 were included in the analysis. Center lines represent median value, box limits indicate the 25^{th} and 75^{th} percentile and whiskers extend from 2.5^{th} to 97.5^{th} percentile. Data was analyzed statistically using the paired t test and **** indicates $p < 0.0001$. (D) Comparison of global RNA synthesis measured by ^{3}H-uracil incorporation in the absence or in the presence of 150 μg/ml rifampicin as a negative control. Points represent individual measurements with the mean and the error bars displaying the standard error of the mean indicated graphically. Data was statistically analyzed using the unpaired t test (* $p = 0.0199$). (E) Comparison of rRNA levels assessed by RT-qPCR in *rel*⁻ relative to wild-type. Points represent individual measurements and the mean and the standard error of the mean are indicated graphically. (F) Comparison of global protein synthesis measured by ^{35}S-methionine incorporation in the absence or in the presence of 200 μg/ml chloramphenicol. Points represent individual measurements and the mean and the standard error of the mean are indicated graphically. (G) Representative images of wild-type and *rel*⁻ cells used for the analysis of cell length and width. The scale bar corresponds to 2 μm. (H) Comparison of cell geometry measurements in wild-type, the *rel*⁻ and the rel^{D297A} cells. Cell length and width were obtained from microscopy images of 150 cells for each strain, and cell volume was calculated as described in Experimental Procedures. Points represent individual measurements, and the mean and the standard error of the mean are indicated graphically. (I) Growth curves of wild-type and the *rel*⁻ strain in constant light conditions (40 μmol photons m^{-2} s^{-1}) in BG-11 medium. Points represent individual measurements. The black and red lines each represent the best fit for exponential growth using regression analysis, and 95% confidence limits are shown in grey. T_d is the doubling time of each strain. (J) Growth curves of wild-type and the *rel*⁻ strain in constant light conditions (18 μmol photons m^{-2} s^{-1}) in BG-11 medium. Points represent the individual measurements, while the black and red line each represents the best fit for exponential growth using regression analysis. T_d is the corresponding value of the doubling time of each strain.

Puszynska and O'Shea Figure S4

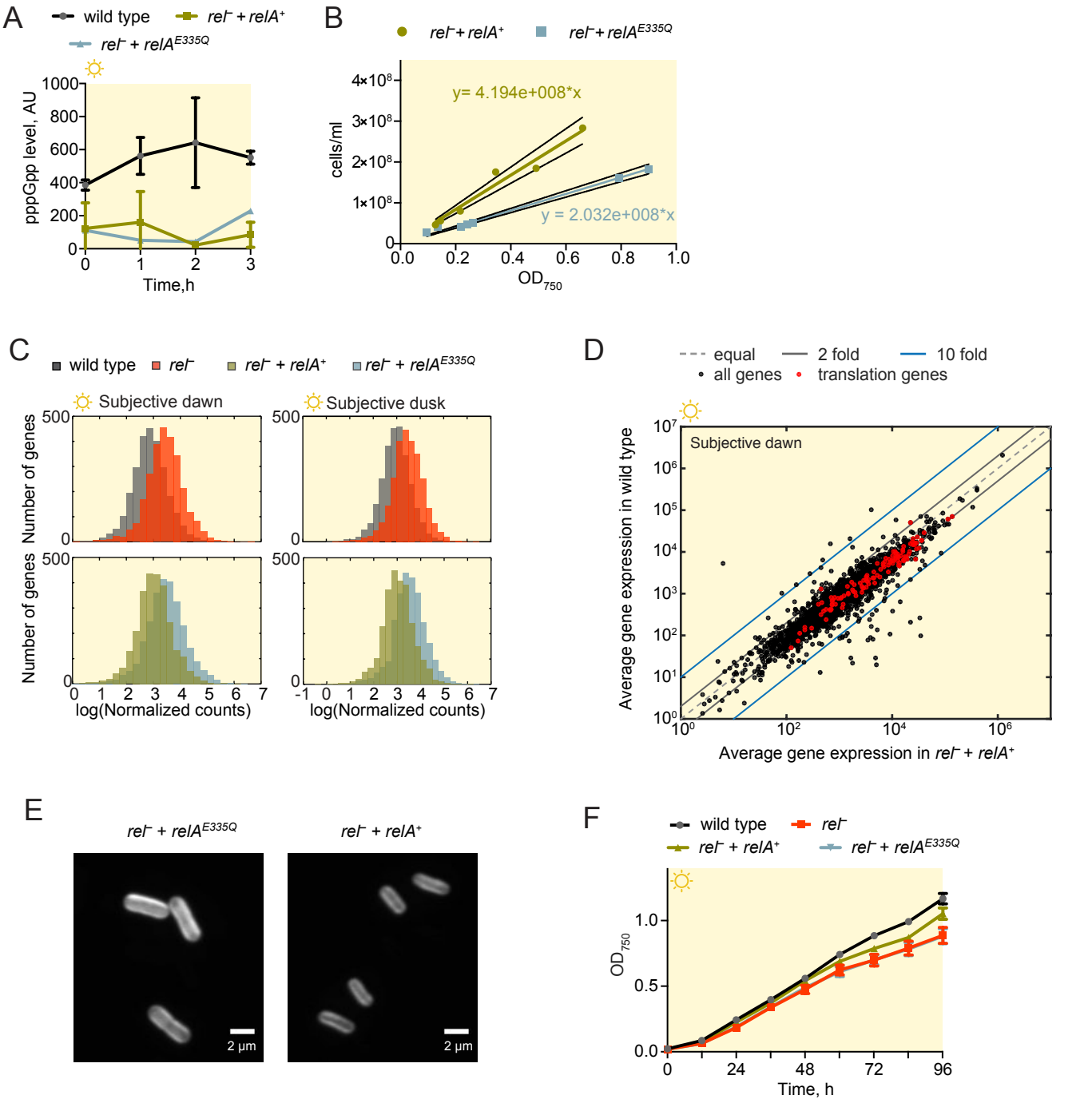

Figure S4. Characterization of the *rel⁻ + relA⁺* and *rel⁻ + relA^{E335Q}* strains in constant light. Related to Figure 3.

(A) pppGpp levels in constant light conditions in the *rel⁻ + relA⁺* strain, the *rel⁻ + relA^{E335Q}* strain, and in wild-type. Points represent the mean of two experiments with error bars displaying the standard error of the mean. (B) Relationship between cell number per ml and OD_{750} for the *rel⁻ + relA⁺* and the *rel⁻ + relA^{E335Q}* strains. Points represent individual measurement, while the blue and green lines correspond to the best fit lines obtained using linear regression analysis. 95% confidence limit bands are shown using black lines. Equations describing the relationship between cell number per ml and OD_{750} the *rel⁻ + relA⁺* and the *rel⁻ + relA^{E335Q}* strains are represented in green and blue respectively. (C) Histograms of log10 transformed normalized sequencing counts for all genes at subjective dawn and at subjective dusk in wild-type, the *rel⁻*, *rel⁻ + relA⁺* and *rel⁻ + relA^{E335Q}* strains. (D) Scatter plots comparing gene expression levels between wild-type and the *rel⁻ + relA⁺* strain at subjective dusk highlighting the genes involved in translation. Points represent mean expression values for all genes obtained in two biological replicates. Translation genes are indicated in red. Equal expression and the cutoffs for 2-fold and 10-fold expression changes are indicated graphically with diagonal lines. (E) Representative images of the *rel⁻ + relA⁺* and the *rel⁻ + relA^{E335Q}* cells used in the analysis of cell length and width. The scale bar corresponds to 2 μm. (F) Growth curves of wild-type, the *rel⁻*, the *rel⁻ + relA⁺* and the *rel⁻ + relA^{E335Q}* strains in constant light conditions (40 μmol photons m^{-2} s^{-1}) in BG-11 medium. Points represent the mean of seven biological replicates with error bars displaying the standard error of the mean.

Puszynska and O'Shea Figure S5

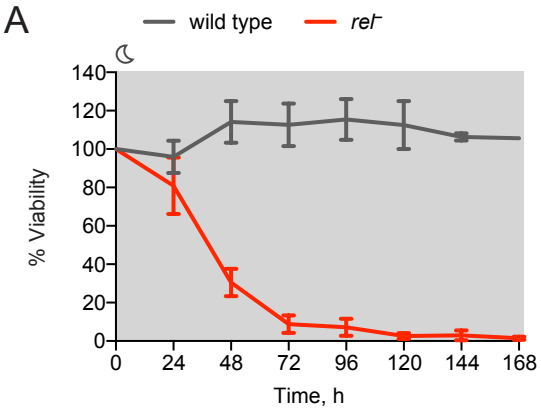

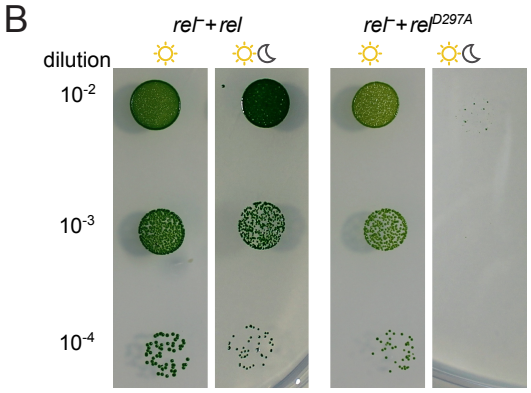

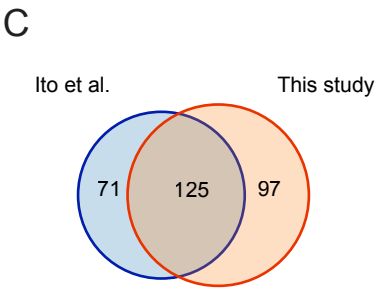

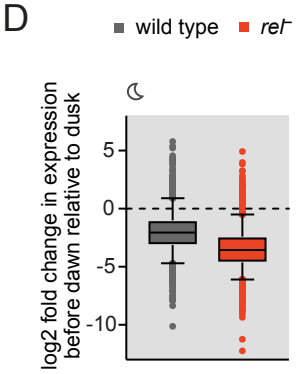

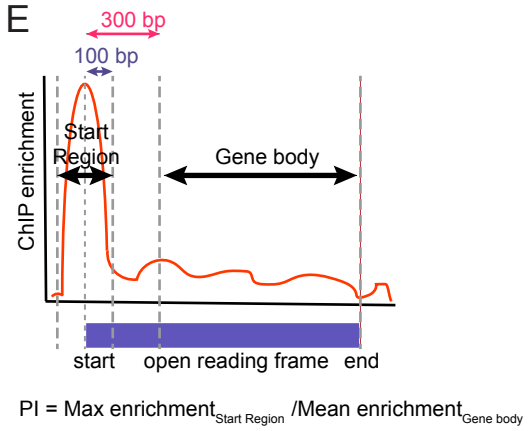

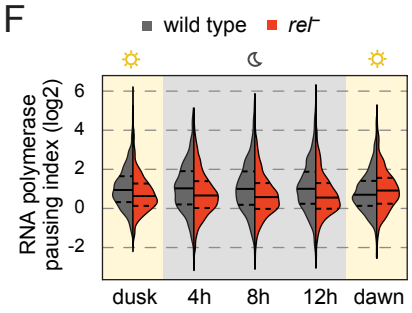

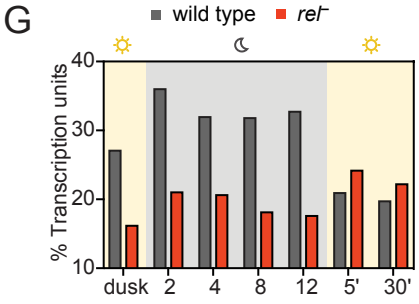

Figure S5. Characterization of the *rel* mutant strains in light/dark conditions. Related to Figure 4
(A) Viability of wild-type and the *rel*⁻ strain after prolonged incubation in darkness. The survival of cells was assessed by a colony forming unit assay. Points represent the mean of two experiments for wild-type and six experiments for the *rel*⁻ strain with error bars displaying the standard error of the mean. (B) Comparison of growth of *rel*⁻ strain complemented with either the *rel* gene or rel^{D297A} mutant, using a plate-based assay. The experiment was performed three independent times and a representative experiment is shown. (C) Venn diagram representing the number of dark-induced genes in wild-type detected by Ito et al., 2009, and in this study. (D) Box plots comparing log2 transformed fold change in expression of all genes at the end of darkness (time = 12 h in the dark) relative to their respective expression at dusk in wild-type and the *rel*⁻ mutant. Center lines represent median value, box limits indicate the 25th and 75th percentile and whiskers extend from 5th to 95th percentile. (E) Schematic diagram illustrating calculation of the polymerase pausing index. The RNA polymerase pausing index is defined as the ratio between the maximum enrichment at the start of the transcription unit and the mean RNA polymerase enrichment within the gene body (300 bp from the start of the transcription unit to the end of it). (F) Comparison of distribution of log2 transformed RNA polymerase pausing index in wild-type and the *rel*⁻ strain measured by RNA polymerase chromatin immunoprecipitation followed by sequencing. Solid lines represent the median and the dashed lines the 25th and 75th quartiles of the distribution. (G) Occurrences of the transcription units with a proximally paused polymerase in wild-type and the *rel*⁻ strain over time. Transcription units with a proximally paused polymerase are defined as transcription units characterized by the RNA polymerase pausing index greater than 3.

Puszynska and O'Shea Figure S6

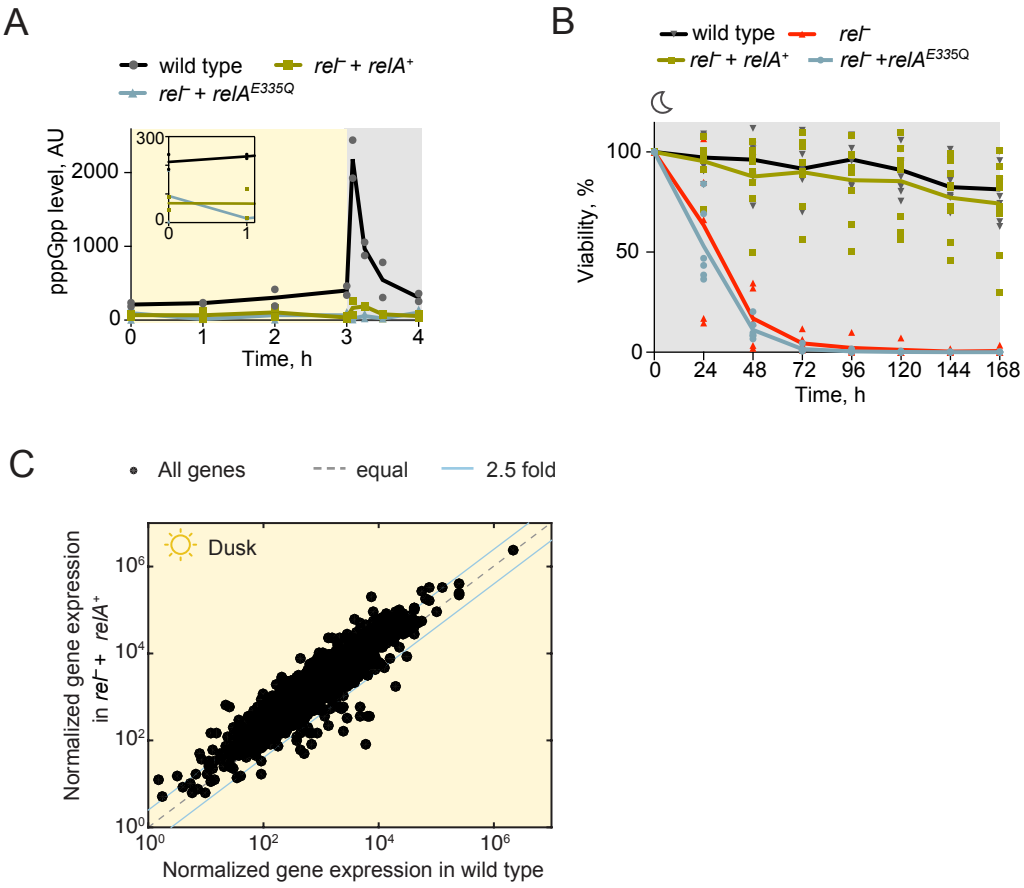

Figure S6. Characterization the *rel⁻ + relA⁺* and the *rel⁻ + relA^{E335Q}* strains in the dark and in light/dark conditions. Related to Figure 5.

(A) pppGpp levels in light and after exposure to darkness in the *rel⁻ + relA⁺* and the *rel⁻ + relA^{E335Q}* strains and in wild-type. Points represent individual measurements and the lines represent the mean of two experiments. The inset shows a magnified view of pppGpp levels in light. (B) Viability of wild-type, the *rel⁻* and the *rel⁻ + relA⁺* and the *rel⁻ + relA^{E335Q}* strains after prolonged incubation in darkness. The survival of cells was assessed by a colony forming unit assay. Points represent biological replicates and lines represent the mean. (C) Scatter plot comparing gene expression levels in wild-type and the *rel⁻+ relA⁺* mutant at dusk. Equal expression and the cutoffs for 2.5-fold expression changes are indicated graphically with diagonal lines.

Supplemental Experimental Procedures
Strain construction

All plasmids used for strain construction were made by Gibson assembly (Gibson et al., 2009). All strains were constructed following standard protocols for genomic integration by homologous recombination (Clerico et al., 2007). All mutant strains were made on a regular basis by fresh transformations, phenotypically verified and used for no longer than 3 weeks to prevent suppressor mutations from arising. To confirm target integration into the genome all strains were analyzed using colony PCR. Strains carrying point mutations introduced in the *rel* or *relA* open reading frames were further verified by PCR amplification of the relevant gene followed by Sanger sequencing.

The *rel*⁻ strain was made by transforming wild-type cells with a pBR322 plasmid carrying a kanamycin resistance cassette, flanked by 1000 nucleotides of DNA from upstream and downstream of the *rel* locus (*synpcc7942_1377*). The *rel*⁻ + *rel* and the *rel*⁻ + rel^{D297A} strains were made by transforming wild-type cells simultaneously with the *rel*⁻ plasmid and with an NS 1 targeting vector pAM1303 carrying either the *rel* gene with its native promoter encompassing 500 base pairs upstream of the translation start, or the analogous rel^{D297A} variant. The rel^{D297A} variant was made by introducing a point mutation inactivating the Rel synthetase activity (following Hogg et al., 2004), using the QuikChange II site directed mutagenesis kit (Agilent) with primers GAGTTCCACGAAATTTTTGCTGTAGCAGCGCTGCGG and CCGCAGCGCTGCTACAGCAAAAATTTCGTGGAACTC. Wild-type strains with the inducible expression of RelA⁺ or $RelA^{E335Q}$ were made by transforming wild-type cells with an NS 1 targeting vector pAM1303 carrying either a constitutively active FLAG-tagged *relA*⁺ construct, whose expression is controlled by a theophylline-responsive riboswitch (Nakahira et al., 2013), or an analogous $relA^{E335Q}$ variant deficient in (p)ppGpp synthetase activity. The *relA*⁺ and $relA^{E335Q}$ constructs were prepared following Gonzalez and Collier (Gonzalez and Collier, 2014). The *rel*⁻ + *relA*⁺ and *rel*⁻ + $relA^{E335Q}$ strains were made by transforming wild-type cells simultaneously with the *rel*⁻ plasmid and with the NS 1 targeting vector pAM1303 carrying either a constitutively active FLAG-tagged *relA*⁺ construct, whose expression is controlled by a theophylline-responsive riboswitch, or the $relA^{E335Q}$ variant. In the experiments with the *rel*⁻ + *relA*⁺ and *rel*⁻ + $relA^{E335Q}$ strains we utilized a low level, leaky expression of *relA*⁺ and $relA^{E335Q}$ in the absence of the inducer.

Growth and viability assays
For the liquid growth assays, liquid cultures of wild-type and mutant cells were pre-grown in continuous light in BG-11 medium with no antibiotics. Cultures were diluted to OD_{750} = 0.015 and grown in constant light at 30 °C. Optical density of cells was monitored every 12 h at OD_{750}.

For the plate assays, liquid cultures of wild-type and mutant cells were pre-grown in continuous light in BG-11 medium with no antibiotics. Cultures were diluted to OD_{750} = 0.25 and then a dilution series was performed from 10^0 to 10^{-4}. 10 µl of each dilution step were spotted onto BG-11 agar plates with no antibiotics and incubated in constant light at 30 °C for 7 days or under 12 h light/ 12 h dark conditions for 14 days.

A colony-forming unit (CFU) assay was performed to assess viability after prolonged dark treatment. Cultures pre-grown in light were diluted to OD_{750} = 0.025 and placed in darkness. Aliquots were removed from cultures every 24 h and diluted 1000-fold in BG-11 medium. Following the dilution, 100 µl of samples were plated in duplicate onto BG-11 plates with no antibiotics. Plates were incubated for 7 days in constant light at 30°C and colonies were counted. Viability was expressed as: % viability = N/N_0 x 100%, where N_0 is the colony count before exposure of cultures to darkness.

Preparation of exogenous RNA standards

Sequences of the standards
>bub2
ATGACCTCAATTGAAGATCTGATATCAAATCCTCCCCTGCTACTGCATTCCTCACTCTCTCAAC
TTCGCTACCTCATACTCAGTGAAGGGCTTCCCATATCTGAAGATAAACAGCAGCAGCGCACGC

GATGTTACGTGTGGACGGTGCTCTCTCAAACTTCTATGGAGGCGTCTACACAACGGTACCTTG
CGCTCTTGAAACTGGGCCCACCTTCCACAACCATTTACCAAAAAATCAAGAACGACACATCCA
GAACTTTTCAGACGGATCCAAACTTTAGAAATAGAGTCTCAGAGGATGCCCTCATCCGGTGTC
TGTCGTGCTTTGCTTGGCAAACACAACAAAGAAGACAAAAGACTCGTTTTGGTCGCATTCCTG
TGAGCACATATGTGCAGGGCATGAACGTGTTATTAGCTCCTCTGCTTTACTCATGTCCTTCTGA
ACCTATGGCGTATCAACTTTTCACTAAGCTTTGTTATGAAATGATACCGACGTATCTAACTAAG
AACCTAAACGGCGCCCAGAACGGCGCCAAACTACTAGATATTTCTCTCAGAATCATTGATCCA
AAGCTGAGTAAATTTCTATCGGACAATTTACTTACAGCAGAGATTTATGGTATGCCTTCCATA
CTCACGTTATCCAGCTGCAATAAACCGCTTGATCAGGTCATTAAACTGTGGGATTTCATGTTTG
CATATGGATTCCATATGAATATTCTCTTTGTGGTGGCATTCCTAGTTAAAATGAGATCCAAGGT
TTTCAAATCGGATTCCCCTGTTAATTTACTACGACAGTTTCCGGATTTTGATGCTGACGAGATC
ATTCGGCTGGGCGTCGGGTTCATCGCTAAGATCCCTGCTCAAATTTATGACCTATTGGTAGAC
CACTTGACCGACCCAGACATATATATACCGTAA

>mam1
ATGAGGGAAAAAAGAACAATTTCAAATAAAGACACAAACTATCTCAAATTCCCAAATAAACT
CCAAAGATATTCCCGATTCTTGAGCAGGAAGATATCCAATACCAGCCCAGAAAAGCAACCGA
AGAAGAACATAAAAGAACACTGTTTATCGAGTTATCATAAAGAACACTCGGTAAAACCAAAG
CAAAACTCCGGTAATGTTGCAGCAAAAGAAGACAAAGATACGCAGCATTTACAAAATAATGT
CGCTAATGAAGAAGCAACGGAATGTCTAACAAGAAGTAATTTGAAAAAGTTACAAGAGAAAA
TTTTCGATAGAGAACTTAATGATATTGCCTGTGATCATTGTCTTTGTAGCACAGAAAATAGAA
GAGATATCAAGTATTCACGACTTTGGTTCCTTTTTGAGTTGGAAATGAGTGAAAACTGGAATG
AAAATCTCCGCCTTAGTTGCTATAATAAATATGTGTATTCCGCAATTGATGAGTCGTGGAAAA
TGGAGAATATTCTACTTAAAGAACAAGAGAAGCATTATGAATATTTTCCAATAGGACAATTAC
TGATACCCAATAATATTGACTACACTAATAAACAGAAAAGGAAGGAAAACATTGAAGACTTA
ACAATTGAAATTGATAGTATTATAGAGACAAACCATCAAAAGAAAAGATTTTTGCCGCAAAG
TGTCCTGATAAAAAGGGAGGATGAAATTGCATTTGACGACTTTCATTTGGATGCACGAAAGGT
TCTAAACGATTTGAGCGCCACTTCTGAAAATCCATTCAGCTCTTCACCAAATACAAAAAAAAT
TAAATCAAAGGGAAAAACCTTGGAAGTGGTTCCCAAAAAGAAAAACAAAAAGATCATAGGT
GCTTTGGAAAGAAAGCTACATATAGATGAAAATTAA

>nyv1
ATGAAACGCTTTAATGGTATGTATAAATATTTCTACACAATTAACAAATGTTTAAAAAAGGGA
TTATGCGAATGCTCATCCCCCCATGCCATAATTTTACTATGTTACATTCAGTAGACTAACGTTC
CATTTTGCTTGATTTTGCATATGGTCTTAGTAAGTTATGTGGAAGTTATAAAAAATGGTGAAAC
AATATCTAGTTGTTTCCAGCCGTTCCAGAAAAACGAAAACTATGGTACAATAACTTCAGCAAA
CGAGCAGATAACGCCGGTCATTTTCCATAATTTGATCATGGATATGGTATTACCCAAAGTAGT
TCCGATCAAGGGGAACAAAGTTACCAAGATGTCAATGAATCTCATCGACGGATTCGATTGTTT
CTACTCCACGGATGACCATGACCCCAAAACTGTGTACGTTTGCTTCACATTAGTAGATATGCC
CAAGATTTTGCCCATCAGGATACTAAGTGGGCTGCAGGAATACGAGTCCAACGCTACAAACG
AACTTTTAAGTTCGCATGTAGGTCAAATACTAGACTCTTTCCATGAAGAGCTGGTCGAATACC
GTAACCAAACTTTAAATAGTTCTGGAAATGGCCAATCTAGTAATGGGAATGGTCAGAACACTA
TAAGTGACATCGGGGATGCCACCGAAGACCAAATAAAGGACGTCATCCAGATAATGAACGAT
AACATCGACAAGTTCTTGGAGAGACAAGAAAGAGTTTCTTTATTGGTGGATAAAACTTCCCAA
CTAAATAGCAGCAGTAATAAATTTAGGCGCAAAGCGGTCAATATAAAAGAAATAATGTGGTG
GCAGAAGGTCAAAAATATTACGTTATTAACTTTCACTATTATACTATTTGTAAGTGCTGCTTTC
ATGTTTTTCTATCTGTGGTAA

>pcl9
ATGATTTCTGACTACGATGCTCTTTTGCAATTCAACAAAAAACCTGTTTCGCAAGAAATGATTC
AGTTCTTAGCCACTTCTACTGCTTCCATAATTAAAATCAGGGAAAATAATAATCCAATCCAAG
GATGTCGCCCACCAGACTTATCTATCTTCATTAAAAACGTGGTAATTCAGTCAAATGTTCAAA
CACCAACTTTAATGGCCACATCAGTTTATTTAAACAAACTGAAAAGCGTAATACCAAAAAATG
TGTACGGTATTAACACCACAAGACATCGGATATTTCTCGGATGCTTGATATTAGCTGCCAAAA
CTCTGAACGATTCTTCTCCCTGGAACAAACACTGGACCACGTACACAGAAGGTTTACTCAGAA
TACGTGAGGTGAATACCATCGAACGAGAACTATTAGAATATTTAAATTGGGATGTGAGGATA

ACTACACCGGATTTGATTGATTCTCTTTCTTACTTCCTCGGGCCTATCAAGGAACAACTATTTT
TACAAAGGAGACAAGAAATGCTGTTGTTCAATGCACCAAGTCCCGGCCAACTGAAAGAATAT
ATAAATCATAGAAGACCGGTTTCGCATTCTAGAACTTCTTCTGCTATATCGGTTCCTTCACTGA
CATCCATGGCAACAGTTTCGACAACAGACTCAAGGTCTTCTCTACTGGCAAAATACCAACCGT
CCCTACCGTTGGTGGAATCTGACAACTTCAACAAAAAAAATCATGTGCCGTTAAGGAATAATA
ACGATATCTGTAATAATTTCAGGGCAGAGGAAAACATACACTCAGTAAACCATATTGATGTAA
CAATGGGAAGTTCACCAGTAATGTCGCATAAGCCCACAATTCACCAACGGTTAAATTTTACAA
GGAGGGGCTGGTCATCGTTTTTCAAGCAATAA

>pom34
ATGAAGATTCAGGCGGGCCAATTGGGCCTGGACGATAATGACGTGCCGGGACCATTGCCGGA
CACAGACAGCAAACCCTCATCACAATCACAAAATGACACACCAATGTTTAAATTGGGCAACTT
TGAAAGTCCTGTGCTCAAGGAGCTATCACGGCGAACGGTAAACAAGGAAATGGAGACGCAGA
GAATTATGACAAACGTAATTGCGTTTGCGTTCTGGAACCTGCTGGTGAAGTTCATCAAGTTCTT
TTGGAACAACACTCATGTTGGGAGACAGTTTTGCAACCGGCTATCCAGAATCCATCTGTACAT
GTTGACATTTCACACGTTAAAGAAGGCTAACATCATATATCACACCACGTTCAGTTGGTTGAA
TGCAGAACTTCTTGACTACTTGTTCCACCTATTAATCTCGCTCAATATACTGTTTTCTCTTTGGA
AGCTCTTATCCACCGTCAAAGTAAGTGATTTGAATCTCACTGACAGGCAAAAGAAGCTCCTGG
GGGTAGACATGCAATCATCTGTCGATACTGGGTTGCAGCCACAACACCCCCACTACGTATCCA
CTTCTAAGATCAGCCAAATGGCACAGAACAAAACACATATTCCTCAAACAAATCTCAAAAAT
CATCCAGCATATCTCTTCAAAGGCTTAGAGACGCCTTTGAAAGCAAGACAAAGGGAAATGGC
GGAGGAACAGACGAAACTACAATCTCAATCCTTACACACAAAGAATGTATTTGGCACACTGC
AGAGGCATAGCGGTATCAGTAGCACATTAGTGAGCGCTAACAATGACAATAACTCGCCGCAT
ACCCCTGTAACTAGGAAGGGCTACATTCCAAGTAGCAAATATGCATATATGATGAACTCACAG
TCCCCAAGGGGGAAAATATAA

>uba3
ATGGACTGCAAGATATTGGTGTTAGGCGCAGGTGGTCTAGGATGCGAAATCCTGAAGAATTTG
ACAATGTTAAGCTTTGTTAAACAGGTTCATATTGTAGATATAGACACAATCGAGCTAACCAAC
CTTAATAGACAATTTCTTTTTTGTGATAAGGACATAGGCAAACCGAAAGCTCAAGTGGCAGCC
CAGTATGTAAACACGCGGTTCCCTCAATTGGAAGTTGTGGCGCACGTACAGGACCTGACCACT
TTGCCCCCGAGCTTTTACAAAGACTTCCAGTTCATAATCTCGGGGCTGGACGCCATTGAACCT
CGTCGCTTCATCAATGAGACTCTCGTGAAGCTTACCTTGGAGTCCAATTATGAAATTTGCATCC
CGTTCATAGATGGTGGAACAGAGGGGCTCAAGGGACATGTAAAAACAATCATTCCAGGCATC
ACTGCATGCTGGGAGTGCTCCATTGATACCTTGCCCTCGCAGCAGGATACTGTGCCAATGTGT
ACAATCGCCAACAATCCTCGCTGCATTGAGCATGTTGTGGAGTATGTCTCAACTATACAATAC
CCTGATTTAAATATTGAGTCTACGGCGGATATGGAATTTCTGCTGGAGAAGTGCTGCGAAAGG
GCTGCCCAATTTAGCATCTCAACAGAAAAATTATCAACAAGTTTTATCCTGGGTATAATAAAG
AGTATCATACCTAGTGTAAGCACTACGAATGCGATGGTTGCAGCGACATGCTGTACGCAGATG
GTTAAGATTTATAATGATTTAATCGACCTGGAAAACGGCAATAATTTCACTTTGATTAACTGCT
CAGAAGGGTGTTTTATGTACAGTTTCAAGTTCGAGCGGTTACCCGACTGTACTGTTTGTTCAAA
TTCCAATTCCAACTAG

The list of primers used to amplify the RNA standards

Primer name	Primer sequence
bub2_F	GCCAGTGAATTGTAATACGACTCACTATAGGGATGACCTCAATTGAAGATCTGA
bub2_R	TTACGGTATATATATGTCTGGG
mam1_F	GCCAGTGAATTGTAATACGACTCACTATAGGGATGAGGGAAAAAAGAACAATTTC
mam1_R	TTAATTTTCATCTATATGTAGC
nyv1_F	GCCAGTGAATTGTAATACGACTCACTATAGGGATGAAACGCTTTAATGGTATG
nyv1_R	TTACCACAGATAGAAAAACATGAAAGC
pcl9_F	GCCAGTGAATTGTAATACGACTCACTATAGGGATGATTTCTGACTACGATGCTC
pcl9_R	TTATTGCTTGAAAAACGATGACC
pom34_F	GCCAGTGAATTGTAATACGACTCACTATAGGGATGAAGATTCAGGCGGGCC
pom34_R	TTATATTTTCCCCCTTGGGG
uba3_F	GCCAGTGAATTGTAATACGACTCACTATAGGGATGGACTGCAAGATATTGGTG
uba3_R	CTAGTTGGAATTGGAATTTGAAC

Primers used in RT-qPCR analysis of gene expression.

Target	Primer sequences
23S	F: CTGCACCAGAGAAGGTGAAA R: TAGCCTTACGAGGTGGTCCT
16S	F: CAACCTCATACAGGCAATGG R: CGCTGGTGTTCTTCCAGATA
uba3 (S. cerevisiae)	F: CACAATCGAGCTAACCAACC R: CACAACTTCCAATTGAGGGA
bub2 (S. cerevisiae)	F: CCTTCCACAACCATTTACCA R: AAGCAAAGCACGACAGACAC

Chromatin immunoprecipitation

50 ml of cells at OD_{750} equal to 0.2 were cross-linked with 1% formaldehyde for 15 min and quenched with 125 mM glycine for 5 min. Cells were collected by centrifugation for 15 minutes at 4,000 x g at 4°C and washed twice with ice-cold phosphate-buffered saline. Samples were resuspended in 500 µl phosphate-buffered saline and pelleted for 5 min at 3,000 x g. The pellets were flash frozen and stored at -80 °C. Samples were thawed and resuspended in 270 µl of lysis buffer (50 mM HEPES-NaOH pH 7.5, 140 mM NaCl, 1 mM EDTA, 1% Triton X-100, 0.1% sodium deoxycholate, 1x Roche Complete EDTA-free Protease Inhibitors). Cells were disrupted by 10 cycles of 30 sec bead-beating at 4 °C with 0.1 mm glass beads with periodic cooling on ice. Chromatin was sheared by sonication to a median length of ~300 bp. Lysates were then clarified by two rounds of centrifugation at 21,000 x g for 15 min at 4 °C. Protein concentration was determined by BCA assay (Pierce Biotechnology) with a standard curve prepared with Bovine Serum Albumin. 750 µg of lysate from each time point (prepared in 500 ml of the lysis buffer) were mixed with 18 µg of purified anti-*E. coli* RNA polymerase β monoclonal antibody (BioLegend). Samples were incubated overnight at 4 °C with continuous rotation. 70 µl of 1:1 mix of rProtein A Sepharose and Protein G Sepharose Fast Flow beads (GE Healthcare; 50% slurry in the lysis buffer) were added to each sample. Further steps were carried out exactly as detailed in Markson et al., 2013. After 2 h of incubation, beads were isolated by centrifugation for 1 min at 1000 g, washed twice with lysis buffer, once with wash buffer (10 mM Tris-HCl pH 8.0, 250 mM LiCl, 1 mM EDTA, 0.5% NP-40, 0.1% sodium deoxycholate) and once with TE pH 7.5 (10 mM Tris-HCl pH 7.5, 1 mM EDTA). Elution of protein-DNA complexes was performed with 250 µl elution buffer (50 mM Tris-HCl pH 8.0, 10 mM EDTA, 1% SDS) for 1 h at 65 °C.

Crosslinks were reversed by incubation of samples at 65 °C for 12 h. Proteins were digested with proteinase K for 2 h at 37 °C, and samples were extracted with phenol/chloroform/isoamyl alcohol. Nucleic acids were precipitated with ethanol overnight and RNA was digested in 50 µl of TE containing 20 ng/µl of DNase-free RNase (Fermentas). Samples were extracted again with phenol/chloroform/isoamyl alcohol, precipitated with ethanol and resuspended in 50 µl 10 mM Tris-HCl pH 8.0.

ChIP-Seq Library Preparation and Sequencing

Libraries for Illumina sequencing of ChIP DNA were prepared following a protocol developed by Ethan Ford (http://ethanomics.files.wordpress.com) with modifications as described in Markson et al., 2013.

ChIP-seq data analysis

Sequence tags were aligned to the genome using Bowtie (allowing uniquely mappable reads with a maximum of three mismatches to map to the genome). Reads were then counted, extended by 50 bp (the sequence tag length), and normalized between samples. The RNA polymerase pausing index was calculated as the ratio between the maximum enrichment at the start of the transcription unit and the mean RNA polymerase enrichment within the open reading frame (300 bp from the start of the transcription unit to the end of it). Transcription units with a proximally paused polymerase were defined as transcription units characterized by the RNA polymerase pausing index greater than 3. Transcription units used in the analysis are at least 1000 bp long and include operons listed in OperomeDB database (Chetal and Janga, 2015) and single genes (Vijayan et al., 2011).

Supplemental References

Chetal K, Janga SC. (2015). OperomeDB: a database of condition-specific transcription units in prokaryotic genomes. Biomed Res Int. 2015:318217.

Clerico, E.M., Ditty, J.L., Golden, S.S. (2007). Specialized techniques for site-directed mutagenesis in cyanobacteria. Methods Mol. Biol. 362:155–171.

Gibson, D.G., Young, L., Chuang, R.Y., Venter, J.C., Hutchison, C.A. 3rd, Smith, H.O. (2009). Enzymatic assembly of DNA molecules up to several hundred kilobases. Nat Methods. 6:343–5.

Gonzalez D, Collier J. (2014). Effects of (p)ppGpp on the progression of the cell cycle of *Caulobacter crescentus*. J. Bacteriol. 196, 2514–2525.

Huang, D.W., Sherman, B.T., Lempicki, R.A. (2009). Bioinformatics enrichment tools: paths toward the comprehensive functional analysis of large gene lists. Nucleic Acids Res. 37:1-13.

Huang, D.W., Sherman, B.T., Lempicki, R.A. (2009). Systematic and integrative analysis of large gene lists using DAVID Bioinformatics Resources. Nature Protoc. 4:44-57.

Nakahira, Y., Ogawa, A., Asano, H., Oyama, T., and Tozawa, Y. (2013). Theophylline-dependent riboswitch as a novel genetic tool for strict regulation of protein expression in cyanobacterium *Synechococcus elongatus* PCC 7942. Plant Cell Physiol 54: 1724–1735.